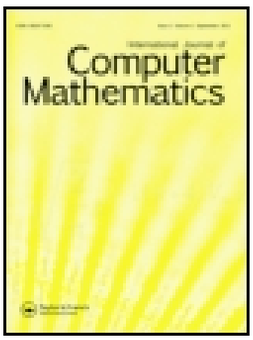

International Journal of Computer Mathematics

ISSN: 0020-7160 (Print) 1029-0265 (Online) Journal homepage: http://www.tandfonline.com/loi/gcom20

Local discontinuous Galerkin methods based on the multisymplectic formulation for two kinds of Hamiltonian PDEs

Wenjun Cai , Yajuan Sun, Yushun Wang & Huai Zhang

To cite this article: Wenjun Cai , Yajuan Sun, Yushun Wang & Huai Zhang (2017): Local discontinuous Galerkin methods based on the multisymplectic formulation for two kinds of Hamiltonian PDEs, International Journal of Computer Mathematics, DOI: 10.1080/00207160.2017.1335866

To link to this article: http://dx.doi.org/10.1080/00207160.2017.1335866

Accepted author version posted online: 29 May 2017.
Published online: 11 Jun 2017.

INTERNATIONAL JOURNAL OF COMPUTER MATHEMATICS, 2017
https://doi.org/10.1080/00207160.2017.1335866

Taylor & Francis
Taylor & Francis Group

ARTICLE

Local discontinuous Galerkin methods based on the multisymplectic formulation for two kinds of Hamiltonian PDEs

Wenjun Cai [a], Yajuan Sun[b], Yushun Wang[a] and Huai Zhang[c]

[a]Jiangsu Provincial Key Laboratory for NSLSCS, School of Mathematical Sciences, Nanjing Normal University, Nanjing, China; [b]LSEC, Academy of Mathematics and Systems Science, Chinese Academy of Sciences, Beijing, China; [c]Key Laboratory of Computational Geodynamics, University of Chinese Academy of Sciences, Beijing, China

ABSTRACT

This paper examines the novel local discontinuous Galerkin (LDG) discretization for Hamiltonian PDEs based on its multisymplectic formulation. This new kind of LDG discretizations possess one major advantage over other standard LDG method, which, through specially chosen numerical fluxes, states the preservation of discrete conservation laws (i.e. energy), and also the multisymplectic structure while the symplectic time integration is adopted. Moreover, the corresponding local multisymplectic conservation law holds at the units of elements instead of each node. Taking the nonlinear Schrödinger equation and the KdV equation as the examples, we illustrate the derivations of discrete conservation laws and the corresponding numerical fluxes. Numerical experiments by using the modified LDG method are demonstrated for the sake of validating our theoretical results.

ARTICLE HISTORY
Received 12 February 2017
Revised 30 March 2017
Accepted 21 April 2017

KEYWORDS
Multisymplectic formulation; Hamiltonian PDEs; local discontinuous Galerkin method; numerical flux; conservation law

2010 AMS SUBJECT CLASSIFICATIONS
35L65; 37K05; 65M20; 65M22; 65M60

1. Introduction

Many conservative types of partial differential equations (PDEs) raised in physics such as meteorology and weather prediction, nonlinear optics, solid mechanics and elastodynamics, oceanography, cosmology, and quantum field theory [5], can be expressed as

$$\boldsymbol{M}\boldsymbol{z}_t + \boldsymbol{K}\boldsymbol{z}_x = \nabla_{\boldsymbol{z}} S(\boldsymbol{z}), \quad \boldsymbol{z} \in \mathbb{R}^d, \ (x,t) \in \mathbb{R}^2, \tag{1}$$

where $\boldsymbol{M}$, $\boldsymbol{K}$ are two skew-symmetric matrices on $\mathbb{R}^d$ ($d \geq 3$) and $S : \mathbb{R}^d \to \mathbb{R}$ is a smooth function. The reformulation for the conservative systems was firstly proposed by Marsden *et al.* [24], and also Bridges and Reich [3] under the concept of multisymplectic geometry which can be viewed as a generalization of the symplectic structure [18]. It is investigated easily that the multisymplectic Hamiltonian system (1) admits the multisymplectic conservation law [17]

$$\partial_t(\mathrm{d}\boldsymbol{z} \wedge \boldsymbol{M}\,\mathrm{d}\boldsymbol{z}) + \partial_x(\mathrm{d}\boldsymbol{z} \wedge \boldsymbol{K}\,\mathrm{d}\boldsymbol{z}) = 0, \tag{2}$$

the energy conservation law

$$\partial_t(S(\boldsymbol{z}) + \boldsymbol{z}_x^{\mathrm{T}}\boldsymbol{K}_+\boldsymbol{z}) + \partial_x(-\boldsymbol{z}_t^{\mathrm{T}}\boldsymbol{K}_+\boldsymbol{z}) = 0, \tag{3}$$

and the momentum conservation law

$$\partial_t(-\boldsymbol{z}_x^{\mathrm{T}}\boldsymbol{M}_+\boldsymbol{z}) + \partial_x(S(\boldsymbol{z}) + \boldsymbol{z}_t^{\mathrm{T}}\boldsymbol{M}_+\boldsymbol{z}) = 0, \tag{4}$$

CONTACT Wenjun Cai caiwenjun@njnu.edu.cn Jiangsu Provincial Key Laboratory for NSLSCS, School of Mathematical Sciences, Nanjing Normal University, Nanjing 210023, China; Huai Zhang huaizhang@gmail.com Key Laboratory of Computational Geodynamics, University of Chinese Academy of Sciences, Beijing 100049, China

where $\boldsymbol{M} = \boldsymbol{M}_+ - \boldsymbol{M}_+^{\mathrm{T}}$, $\boldsymbol{K} = \boldsymbol{K}_+ - \boldsymbol{K}_+^{\mathrm{T}}$. Notice that the local conservation laws (3) and (4) are expressed slightly different from the standard cases [3] in order to ensure that these conservation laws can coincide with ones in physics under the proper splittings of M and K which is probably not unique. Given a periodic boundary condition (or zero boundary condition), the global conservation laws can be derived by integrating Equations (3) and (4) along the spatial direction.

It is considered that the elaborately designed numerical algorithms which are able to preserve the corresponding conservation laws inherited by the given system, usually exhibit remarkable stability over long-time duration [18]. Multisymplectic integrators are designed based on the construction principle. They are proposed aiming to preserve a discrete version of the multisymplectic conservation law (2). To date, such integrators have been widely applied on various Hamiltonian PDEs including the wave equations [16,26], the nonlinear Schrödinger (NLS) equation [20,27], the KdV equation [1,31,38], Maxwell's equation [6,21,28], the Camassa–Holm equation [15,40], and so on. In order to establish the multisymplectic integrators, some existing techniques on spatial discretization can also been employed, for examples, the (partitioned) Runge–Kutta method [19,26], the spectral [4] or pseudo-spectral method [8], the wavelet collocation method [39,40], etc.

It is well known that the finite-element method (FEM), whose mathematical theory is more profound and complete [9], has great advantages in the flexibility of complex geometry and various kinds of boundary conditions. However, the existing results in the literature for simulating conservative PDEs are rarely focused on the conservative properties of the system by combining the FEM. Therefore, it is worth investigating the efficient structure-preserving schemes, for example, the multisymplectic integrator, in the FEM framework for these systems (1).

Different from the standard FEM, the discontinuous Galerkin (DG) method, recently has received growing concern due to its own merits of high-order accuracy, compact formulation and parallelism. Due to that the DG methods adopt the completely discontinuous piecewise polynomials as the test functions, it is more flexible to incorporate the preservation properties. The DG method is firstly introduced by Reed and Hill [25] in addressing the linear neutron transport problem. Later, it is developed by Cockburn *et al.* in a series of papers [10,11,13,14] for preserving nonlinear conservation laws. Moreover, the local discontinuous Galerkin (LDG) method, which is a variant of DG method, is firstly introduced by Cockburn and Shu [12] to deal with a convection–diffusion equation of the second-order derivatives. It is noticed to be more suitable for solving PDEs with spatial derivatives of high order. This method has been generalized to many PDEs including the NLS equation, the KdV equation, the Camassa–Holm equation, the Degasperis–Procesi equation, etc. (see the review paper [34]).

In the implementation of the LDG method the higher order PDEs need to be reformulated into a set of first-order systems. By choosing the alternating numerical flux, we can derive the LDG discretization with L_2-stable. In order to construct the LDG discretizations which can preserve some conservation properties of the concerned system, we consider the LDG discretizations based on the multisymplectic formulation (1) of the conservative system. In [29] we have investigated geometric properties of the LDG method for Hamiltonian ODEs and PDEs through its connection with the continuous-stage partitioned Runge–Kutta (PRK) method. In this work, taking the NLS equation and the KdV equation for examples, we demonstrate the LDG numerical discretizations by specially choosing the numerical fluxes, LDG schemes do preserve some kinds of conservation laws. Furthermore, if we apply the symplectic discretization in time, these schemes are essentially multisymplectic integrators and preserve some conservation laws over longer time. These methodologies of constructing the LDG method can be easily generalized to other types of Hamiltonian PDEs.

It is noticed that some conservative schemes based on the DG method and its variations have been constructed very recently for the KdV equation [36], the generalized KdV equation [2,23], the Schrödinger-KdV system [32], and the Camassa–Holm equation [22]. In this paper, our construction of LDG methods is based on the multisymplectic formulation of the conservative system. This helps to understand further the resulting numerical discretization.

The rest of this paper is organized as follows. In Section 2, we present the multisymplectic formulations of the NLS and the KdV equations and derive their corresponding LDG discretizations, respectively. The discrete conservation laws are also obtained with specially chosen numerical fluxes. In Section 3, we investigate the multisymplecticity of our LDG schemes in details. The algorithm implementations are also discussed in this section. The numerical experiments by applying the LDG schemes to demonstrate the preservation of conservative quantities and accuracy of numerical methods are given in Section 4. Finally, concluding remarks are obtained in Section 5.

2. LDG spatial discretizations based on multisymplectic formulations

In this section, we discuss the LDG discretizations for the NLS and the KdV equations based on their multisymplectic formulations. For convenience, we introduce the following notations. The computation domain is $\Omega = [a, b]$ which is divided as $I_j = (x_{j-1/2}, x_{j+1/2})$ for $j = 1, 2, \ldots, N$ with the uniform spatial grid $h = x_{j+1/2} - x_{j-1/2}$. The time step is denoted by τ. Denote $t^n = n\tau$ with n an integer. The left and right limits of the discontinuous solution u at cell interface $x_{j+1/2}$ are denoted by $u^{\mp}_{j+1/2} = u(x^{\mp}_{j+1/2}, t)$, thus the central flux is calculated by $u^c_{j+1/2} = (u^+_{j+1/2} + u^-_{j+1/2})/2$ for $j = 1, 2, \ldots, N-1$. We define the piecewise polynomial space V_h by

$$V_h = \{v : v \in P^k(I_j) \text{ for } x \in I_j,\ j = 1, 2, \ldots, N\},$$

which includes the polynomials of degree up to k in each cell I_j.

2.1. Multisymplectic formulation of the NLS equation

We consider the NLS equation

$$\mathrm{i}u_t + u_{xx} + \alpha|u|^2 u = 0, \quad \alpha > 0, \tag{5}$$

where $u(x, t)$ is complex. This equation is an example of a universal nonlinear model that describes many nonlinear physical phenomena. Assuming $u = p + \mathrm{i}q$, we can write the NLS equation (5) in a real-valued form

$$\begin{pmatrix} 0 & -1 \\ 1 & 0 \end{pmatrix} \begin{pmatrix} p \\ q \end{pmatrix}_t + \begin{pmatrix} 1 & 0 \\ 0 & 1 \end{pmatrix} \begin{pmatrix} p \\ q \end{pmatrix}_{xx} + \alpha \begin{pmatrix} q^2 p + p^3 \\ p^2 q + q^3 \end{pmatrix} = 0. \tag{6}$$

In order to derive the multisymplectic formulation of Equation (5), we follow the general approach presented in [7,30]. By deriving the corresponding Lagrangian density from the inverse problem of the calculus of variations, the multisymplectic Hamiltonian system of the NLS equation can be reformed via the covariant Legendre transformation $v = p_x$, $w = q_x$. It is

$$\begin{aligned} q_t - v_x &= \alpha(p^2 + q^2)p, \\ -p_t - w_x &= \alpha(p^2 + q^2)q, \\ p_x &= v, \\ q_x &= w, \end{aligned} \tag{7}$$

which is equivalent to the multisymplectic formulation (1) with

$$\boldsymbol{M} = \begin{pmatrix} 0 & 1 & 0 & 0 \\ -1 & 0 & 0 & 0 \\ 0 & 0 & 0 & 0 \\ 0 & 0 & 0 & 0 \end{pmatrix}, \quad \boldsymbol{K} = \begin{pmatrix} 0 & 0 & -1 & 0 \\ 0 & 0 & 0 & -1 \\ 1 & 0 & 0 & 0 \\ 0 & 1 & 0 & 0 \end{pmatrix}, \quad \boldsymbol{z} = \begin{pmatrix} p \\ q \\ v \\ w \end{pmatrix} \tag{8}$$

and the Hamiltonian function $S(\boldsymbol{z}) = \frac{1}{2}(v^2 + w^2 + (\alpha/2)(p^2 + q^2)^2)$.

It is known that the multisymplectic conservation law for the NLS equation (6) is

$$\frac{\partial}{\partial t}(\mathrm{d}q \wedge \mathrm{d}p) + \frac{\partial}{\partial x}(\mathrm{d}p \wedge \mathrm{d}v + \mathrm{d}q \wedge \mathrm{d}w) = 0. \tag{9}$$

The corresponding energy conservation law is

$$\frac{\partial}{\partial t}\left[\frac{1}{2}\left(\frac{\alpha}{2}(p^2+q^2)^2 - v^2 - w^2\right)\right] + \frac{\partial}{\partial x}(vp_t + wq_t) = 0. \tag{10}$$

Besides the above two properties, the NLS equation admits the charge (normal) conservation

$$\frac{\partial}{\partial t}\left[\frac{1}{2}(p^2+q^2)\right] + \frac{\partial}{\partial x}(pw - qv) = 0. \tag{11}$$

Under the periodic boundary condition, the following global energy and charge conservation laws hold:

$$\begin{aligned} \mathcal{E}(t) &= \frac{1}{2}\int_\Omega \left[\frac{\alpha}{2}(p^2+q^2)^2 - v^2 - w^2\right]\mathrm{d}x = \mathcal{E}(0), \\ \mathcal{C}(t) &= \frac{1}{2}\int_\Omega (p^2+q^2)\,\mathrm{d}x = \mathcal{C}(0). \end{aligned} \tag{12}$$

2.2. Semi-discretization for the NLS equation based on LDG approach

The LDG method for the NLS equation (7) is formulated as follows: find the approximate solutions $p_h, q_h, v_h, w_h \in V_h$ such that for all test functions $\mu, \lambda, \xi, \nu \in V_h$ the following equality holds:

$$\begin{aligned} \int_{I_j}(q_h)_t\mu\,\mathrm{d}x + \int_{I_j} v_h\mu_x\,\mathrm{d}x - (\hat{v}_h\mu^-)_{j+1/2} + (\hat{v}_h\mu^+)_{j-1/2} &= \alpha\int_{I_j}(p_h^2+q_h^2)p_h\mu\,\mathrm{d}x, \\ -\int_{I_j}(p_h)_t\lambda\,\mathrm{d}x + \int_{I_j} w_h\lambda_x\,\mathrm{d}x - (\hat{w}_h\lambda^-)_{j+1/2} + (\hat{w}_h\lambda^+)_{j-1/2} &= \alpha\int_{I_j}(p_h^2+q_h^2)q_h\lambda\,\mathrm{d}x, \\ -\int_{I_j}(p_h)\xi_x\,\mathrm{d}x + (\hat{p}_h\xi^-)_{j+1/2} - (\hat{p}_h\xi^+)_{j-1/2} &= \int_{I_j} v_h\xi\,\mathrm{d}x, \\ -\int_{I_j}(q_h)\nu_x\,\mathrm{d}x + (\hat{q}_h\nu^-)_{j+1/2} - (\hat{q}_h\nu^+)_{j-1/2} &= \int_{I_j} w_h\nu\,\mathrm{d}x, \end{aligned} \tag{13}$$

where $\hat{v}_h$, $\hat{w}_h$, $\hat{p}_h$, and $\hat{q}_h$ are numerical fluxes which are the most crucial part in order to design a stable conservative numerical scheme.

Remark 2.1: To clarify the following discussion, we denote two kinds of choices of numerical fluxes for a pair, e.g. (p_h, v_h): the alternating flux choice, which takes the left and right fluxes alternatively, for example,

$$\hat{p}_h = p_h^+, \quad \hat{v}_h = v_h^- \quad \text{or} \quad \hat{p}_h = p_h^-, \quad \hat{v}_h = v_h^+;$$

and the central flux choice, which adopts both central fluxes

$$\hat{p}_h = p_h^c, \quad \hat{v}_h = v_h^c.$$

Proposition 2.1: *The solution of the LDG scheme for the NLS equation* (13) *satisfies the semi-discrete energy conservation law, which is*

$$\frac{1}{2}\frac{\mathrm{d}}{\mathrm{d}t}\int_{\Omega}\left[\frac{\alpha}{2}(p_h^2+q_h^2)^2-v_h^2-w_h^2\right]=0, \tag{14}$$

if we take either an alternating choice of fluxes for a pair or central fluxes for both, where a pair in this case means (p_h, v_h) *or* (q_h, w_h).

Proof: Let $\mu=(p_h)_t$ and $\lambda=(q_h)_t$ be the test functions in the first two equations of (13), we can obtain

$$\begin{aligned}
&\int_{I_j}(q_h)_t(p_h)_t\,\mathrm{d}x+\int_{I_j}v_h(p_h)_{tx}\,\mathrm{d}x-(\hat{v}_h(p_h)_t^-)_{j+1/2}+(\hat{v}_h(p_h)_t^+)_{j-1/2}\\
&\quad=\alpha\int_{I_j}(p_h^2+q_h^2)p_h(p_h)_t\,\mathrm{d}x,\\
&-\int_{I_j}(p_h)_t(q_h)_t\,\mathrm{d}x+\int_{I_j}w_h(q_h)_{tx}\,\mathrm{d}x-(\hat{w}_h(q_h)_t^-)_{j+1/2}+(\hat{w}_h(q_h)_t^+)_{j-1/2}\\
&\quad=\alpha\int_{I_j}(p_h^2+q_h^2)q_h(q_h)_t\,\mathrm{d}x.
\end{aligned}\tag{15}$$

Taking the time derivatives of the last two equations in (13) and choosing the test functions as $\xi=-v_h$, $\nu=-w_h$, we have

$$\begin{aligned}
&\int_{I_j}(p_h)_t(v_h)_x\,\mathrm{d}x-(\widehat{(p_h)_t}v_h^-)_{j+1/2}+(\widehat{(p_h)_t}v_h^+)_{j-1/2}=-\int_{I_j}(v_h)_tv_h\,\mathrm{d}x,\\
&\int_{I_j}(q_h)_t(w_h)_x\,\mathrm{d}x-(\widehat{(q_h)_t}w_h^-)_{j+1/2}+(\widehat{(q_h)_t}w_h^+)_{j-1/2}=-\int_{I_j}(w_h)_tw_h\,\mathrm{d}x.
\end{aligned}\tag{16}$$

Summing up Equations (15) and (16) and applying the integration by part yield

$$\begin{aligned}
&(v_h^-(p_h)_t^-)_{j+1/2}-(v_h^+(p_h)_t^+)_{j-1/2}+(w_h^-(q_h)_t^-)_{j+1/2}-(w_h^+(q_h)_t^+)_{j-1/2}\\
&-(\hat{v}_h(p_h)_t^-)_{j+1/2}+(\hat{v}_h(p_h)_t^+)_{j-1/2}-(\widehat{(p_h)_t}v_h^-)_{j+1/2}+(\widehat{(p_h)_t}v_h^+)_{j-1/2}\\
&-(\hat{w}_h(q_h)_t^-)_{j+1/2}+(\hat{w}_h(q_h)_t^+)_{j-1/2}-(\widehat{(q_h)_t}w_h^-)_{j+1/2}+(\widehat{(q_h)_t}w_h^+)_{j-1/2}\\
&\quad=\frac{1}{2}\frac{\mathrm{d}}{\mathrm{d}t}\int_{I_j}\left[\frac{\alpha}{2}(p_h^2+q_h^2)^2-v_h^2-w_h^2\right].
\end{aligned}\tag{17}$$

We take the alternating fluxes, for example,

$$\hat{p}_h=p_h^+,\quad \hat{v}_h=v_h^-,\quad \hat{q}_h=q_h^+,\quad \hat{w}_h=w_h^-, \tag{18}$$

then the local energy conservation law is obtained as

$$\begin{aligned}
&(v_h^-(p_h)_t^+)_{j-1/2}-((p_h)_t^+v_h^-)_{j+1/2}+(w_h^-(q_h)_t^+)_{j-1/2}-((q_h)_t^+w_h^-)_{j+1/2}\\
&\quad=\frac{1}{2}\frac{\mathrm{d}}{\mathrm{d}t}\int_{I_j}\left[\frac{\alpha}{2}(p_h^2+q_h^2)^2-v_h^2-w_h^2\right].
\end{aligned}\tag{19}$$

Summing up Equation (19) over j and using the periodic boundary conditions, we can prove the semi-discrete energy conservation law (14). Another choice for the numerical flux can be the central

flux for $(\hat{p}_h, \hat{v}_h)$ and alternate fluxes for $(\hat{q}_h, \hat{w}_h)$, i.e.

$$\hat{p}_h = p_h^c, \quad \hat{v}_h = q_h^c, \quad \hat{q}_h = q_h^+, \quad \hat{w}_h = w_h^-. \tag{20}$$

With Equation (20), we can also derive the semi-discrete energy conservation law. Moreover, taking the central flux for all the variables will also lead to the same result. ■

Proposition 2.2: *The solution of the LDG scheme* (13) *for the NLS equation satisfies the semi-discrete charge* (*normal*) *conservation law, i.e.*

$$\frac{\mathrm{d}}{\mathrm{d}t}\int_\Omega (p_h^2 + q_h^2)\,\mathrm{d}x = 0. \tag{21}$$

if we take either an alternating choice of the fluxes for a pair or central fluxes for both. The pair in this case means (p_h, w_h) *or* (q_h, v_h).

***Proof*:** Taking the test functions in Equation (13) as $\mu = q_h$, $\lambda = -p_h$, $\xi = w_h$, $\nu = -v_h$, and summing up the resulting equations with the use of discrete integration by part, we have

$$\begin{aligned}
&-(v_h^- q_h^-)_{j+1/2} + (v_h^+ q_h^+)_{j-1/2} + (w_h^- p_h^-)_{j+1/2} - (w_h^+ p_h^+)_{j-1/2} \\
&+(\hat{v}_h q_h^-)_{j+1/2} - (\hat{v}_h q_h^+)_{j-1/2} + (\hat{q}_h v_h^-)_{j+1/2} - (\hat{q}_h v_h^+)_{j-1/2} \\
&-(\hat{w}_h p_h^-)_{j+1/2} + (\hat{w}_h p_h^+)_{j-1/2} - (\hat{p}_h w_h^-)_{j+1/2} + (\hat{p}_h w_h^+)_{j-1/2} \\
&\quad = \frac{1}{2}\frac{\mathrm{d}}{\mathrm{d}t}\int_{I_j} (p_h^2 + q_h^2)\,\mathrm{d}x.
\end{aligned} \tag{22}$$

The charge conservation can be derived in a similar way to Proposition 2.1. ■

According to Propositions 2.1 and 2.2, we have the following corollary.

Corollary 2.1: *The solution of the LDG scheme* (13) *for the NLS equation satisfies both the semi-discrete energy conservation law* (14) *and charge conservation law* (21) *if we take one of the following three numerical fluxes*

$$\hat{p}_h = p_h^+, \quad \hat{v}_h = v_h^-, \quad \hat{q}_h = q_h^+, \quad \hat{w}_h = w_h^-, \tag{23}$$

$$\hat{p}_h = p_h^-, \quad \hat{v}_h = v_h^+, \quad \hat{q}_h = q_h^-, \quad \hat{w}_h = w_h^+, \tag{24}$$

$$\hat{p}_h = p_h^c, \quad \hat{v}_h = v_h^c, \quad \hat{q}_h = q_h^c, \quad \hat{w}_h = w_h^c. \tag{25}$$

Remark 2.2: Note that with the choice (24), the LDG scheme (13) is just a simplified version of the scheme proposed in [33] for the generalized Schrödinger equation

$$iu_u + u_{xx} + i(g(|u|^2)u)_x + f(|u^2|)u = 0.$$

Here, we set $g(u) = 0$ and $f(u) = \alpha u$. However, the significance of our current work is to investigate the relations between the choice of numerical flux and the preservation of conservation laws as well as the multisymplecticity of the fully discrete scheme. Since the multisymplectic methods have already been proven that they have superior numerical behaviour in long-term stability and invariant preservation, it will be more powerful if the LDG method can be introduced into the framework of multisymplectic methods. Although here we only discuss the multisymplecticity of the LDG method in one-dimensional cases, it is very promising that such conclusion can be generalized to high-dimensional problems which will be further investigated in our future works.

2.3. Multisymplectic formulation of the KdV equation

In this section, we consider the KdV equation

$$u_t + \eta u u_x + \varepsilon^2 u_{xxx} = 0, \tag{26}$$

where η and ε are real. A direct calculation shows that the KdV equation (26) does not satisfy the symmetry condition[1]. Thus, it is necessary to introduce a potential $\phi_x = u$ with which the KdV equation can be transformed as

$$\phi_{tx} + \eta \phi_x \phi_{xx} + \varepsilon^2 \phi_{xxxx} = 0. \tag{27}$$

This guarantees an existence of Lagrangian function. Thus, via the corresponding covariant Legendre transformation, we obtain

$$v = \varepsilon u_x, \quad w = \frac{1}{2}\phi_t + \varepsilon v_x + \frac{\eta}{2}u^2.$$

Based on the De Donder–Weyl equations, the KdV equation (26) can be rewritten as the following first-order system:

$$\begin{aligned} \frac{1}{2}u_t + w_x &= 0, \\ -\frac{1}{2}\phi_t - \varepsilon v_x &= -w + \frac{\eta}{2}u^2, \\ \varepsilon u_x &= v, \\ -\phi_x &= -u, \end{aligned} \tag{28}$$

which can be further recast as a multisymplectic formulation (1) with

$$\boldsymbol{M} = \begin{pmatrix} 0 & \frac{1}{2} & 0 & 0 \\ -\frac{1}{2} & 0 & 0 & 0 \\ 0 & 0 & 0 & 0 \\ 0 & 0 & 0 & 0 \end{pmatrix}, \quad \boldsymbol{K} = \begin{pmatrix} 0 & 0 & 0 & 1 \\ 0 & 0 & -\varepsilon & 0 \\ 0 & \varepsilon & 0 & 0 \\ -1 & 0 & 0 & 0 \end{pmatrix}, \quad \boldsymbol{z} = \begin{pmatrix} \phi \\ u \\ v \\ w \end{pmatrix}, \tag{29}$$

and $S(\boldsymbol{z}) = \frac{1}{2}v^2 - uw + (\eta/6)u^3$.

Remark 2.3: Different from that of the NLS equation (8), the multisymplectic formulation of the KdV equation (29) includes an extra potential ϕ. The examples include the KP equation, the Camassa–Holm equation, the BBM equation etc.

The corresponding multisymplectic conservation law for the KdV equation (26) is

$$\frac{\partial}{\partial t}\left[\frac{1}{2}(\mathrm{d}\phi \wedge \mathrm{d}u)\right] + \frac{\partial}{\partial x}(\mathrm{d}\phi \wedge \mathrm{d}w + \varepsilon\, \mathrm{d}v \wedge \mathrm{d}u) = 0. \tag{30}$$

The corresponding local energy and momentum conservation laws are

$$\frac{\partial}{\partial t}\left(\frac{\eta}{6}u^3 - \frac{1}{2}v^2\right) + \frac{\partial}{\partial x}(\varepsilon v u_t - w\phi_t) = 0, \tag{31}$$

and

$$\frac{\partial}{\partial t}\left(\frac{1}{2}u^2\right) + \frac{\partial}{\partial x}\left(uw - \frac{1}{2}v^2 - \frac{1}{6}\eta u^3 - \frac{1}{2}u\phi_t\right) = 0, \tag{32}$$

respectively.

Under the periodic boundary condition, the global energy and momentum conservation laws have the forms

$$\mathcal{E}(t) = \int_\Omega \left(\frac{\eta}{6}u^3 - \frac{1}{2}v^2\right) \mathrm{d}x = \mathcal{E}(0), \tag{33}$$

and

$$\mathcal{M}(t) = \frac{1}{2}\int_\Omega u^2 \,\mathrm{d}x = \mathcal{M}(0). \tag{34}$$

Besides the above two conservation laws, the KdV equation also admits the following linear invariant:

$$\mathcal{L}(t) = \int_\Omega u \,\mathrm{d}x = \mathcal{L}(0), \tag{35}$$

which is usually taken as a criteria to judge a numerical scheme.

Remark 2.4: On many occasions $\mathcal{M}(t)$ (34) is called the energy of the KdV equation instead of the momentum here. However in view of the multisymplectic framework, it appears in the momentum conservation law and therefore is denoted by the momentum of the KdV equation hereafter.

2.4. Semi-discrete LDG discretization for the KdV equation

The LDG method for the KdV equation is formulated as follows: find $\phi_h, u_h, v_h, w_h \in V_h$ such that, for all test functions $\mu, \lambda, \xi, \nu \in V_h$ the following equalities hold:

$$\begin{aligned}
\frac{1}{2}\int_{I_j}(u_h)_t\mu \,\mathrm{d}x - \int_{I_j} w_h\mu_x \,\mathrm{d}x + (\hat{w}_h\mu^-)_{j+1/2} - (\hat{w}_h\mu^+)_{j-1/2} &= 0,\\
-\frac{1}{2}\int_{I_j}(\phi_h)_t\lambda \,\mathrm{d}x + \varepsilon\int_{I_j} v_h\lambda_x \,\mathrm{d}x - \varepsilon(\hat{v}_h\lambda^-)_{j+1/2} + \varepsilon(\hat{v}_h\lambda^+)_{j-1/2} &= -\int_{I_j} w_h\lambda \,\mathrm{d}x + \frac{\eta}{2}\int_{I_j}(u_h)^2\lambda \,\mathrm{d}x,\\
-\varepsilon\int_{I_j} u_h\xi_x \,\mathrm{d}x + \varepsilon(\hat{u}_h\xi^-)_{j+1/2} - \varepsilon(\hat{u}_h\xi^+)_{j-1/2} &= \int_{I_j} v_h\xi \,\mathrm{d}x,\\
\int_{I_j}\phi_h\nu_x \,\mathrm{d}x - (\hat{\phi}_h\nu^-)_{j+1/2} + (\hat{\phi}_h\nu^+)_{j-1/2} &= -\int_{I_j} u_h\nu \,\mathrm{d}x.
\end{aligned} \tag{36}$$

Proposition 2.3: *With the constant boundary condition for ϕ_h and periodic boundary conditions for other variables, the solution of the LDG scheme* (36) *for the KdV equation satisfies the semi-discrete energy conservation law which reads*

$$\frac{\mathrm{d}}{\mathrm{d}t}\int_\Omega \left(\frac{\eta}{6}u_h^3 - \frac{1}{2}v_h^2\right) \mathrm{d}x = 0, \tag{37}$$

if we take either an alternating choice of the fluxes for a pair or central fluxes for both, where the pairs of the KdV equation are (u_h, v_h) and (ϕ_h, w_h).

Proof: Let the test functions be $\mu = (\phi_h)_t$ and $\lambda = (u_h)_t$ in the first two equalities of Equation (36). This gives

$$\begin{aligned}
&\frac{1}{2}\int_{I_j}(u_h)_t(\phi_h)_t\,\mathrm{d}x - \int_{I_j} w_h(\phi_h)_{tx}\,\mathrm{d}x + (\hat{w}_h(\phi_h)_t^-)_{j+1/2} - (\hat{w}_h(\phi_h)_t^+)_{j-1/2} = 0,\\
&-\frac{1}{2}\int_{I_j}(\phi_h)_t(u_h)_t\,\mathrm{d}x + \varepsilon\int_{I_j} v_h(u_h)_{tx}\,\mathrm{d}x - \varepsilon(\hat{v}_h(u_h)_t^-)_{j+1/2} + \varepsilon(\hat{v}_h(u_h)_t^+)_{j-1/2}\\
&\quad = -\int_{I_j} w_h(u_h)_t\,\mathrm{d}x + \frac{\eta}{2}\int_{I_j}(u_h)^2(u_h)_t\,\mathrm{d}x.
\end{aligned} \tag{38}$$

Taking the time derivatives of last two equations in (36) and choosing the test functions as $\xi = -v_h$, $\nu = -w_h$, we obtain

$$\begin{aligned}
&\varepsilon\int_{I_j}(u_h)_t(v_h)_x\,\mathrm{d}x - \varepsilon(\widehat{(u_h)_t}v_h^-)_{j+1/2} + \varepsilon(\widehat{(u_h)_t}v_h^+)_{j-1/2} = -\int_{I_j}(v_h)_t v_h\,\mathrm{d}x,\\
&-\int_{I_j}(\phi_h)_t(w_h)_x\,\mathrm{d}x + (\widehat{(\phi_h)_t}w_h^-)_{j+1/2} - (\widehat{(\phi_h)_t}w_h^+)_{j-1/2} = \int_{I_j}(u_h)_t w_h\,\mathrm{d}x.
\end{aligned} \tag{39}$$

Summing up Equations (38) and (39) and using the integration by part give

$$\begin{aligned}
&-\varepsilon(\widehat{(u_h)_t}v_h^-)_{j+1/2} + \varepsilon(\widehat{(u_h)_t}v_h^+)_{j-1/2} + (\widehat{(\phi_h)_t}w_h^-)_{j+1/2} - (\widehat{(\phi_h)_t}w_h^+)_{j-1/2}\\
&+\varepsilon((u_h)_t^- v_h^-)_{j+1/2} - \varepsilon((u_h)_t^+ v_h^+)_{j-1/2} - \varepsilon(\hat{v}_h(u_h)_t^-)_{j+1/2} + \varepsilon(\hat{v}_h(u_h)_t^+)_{j-1/2}\\
&-((\phi_h)_t^- w_h^-)_{j+1/2} + ((\phi_h)_t^+ w_h^+)_{j-1/2} + (\hat{w}_h(\phi_h)_t^-)_{j+1/2} - (\hat{w}_h(\phi_h)_t^+)_{j-1/2}\\
&\quad = \frac{\mathrm{d}}{\mathrm{d}t}\int_{I_j}\left(\frac{\eta}{6}(u_h)^3 - \frac{1}{2}(v_h)^2\right)\mathrm{d}x.
\end{aligned} \tag{40}$$

For the KdV equation, we should be careful about the boundary condition for the potential variable ϕ_h. By definition, it is know that $(\phi_h)_x = u_h$. Integrating this equation over an interval $\Omega = [a, b]$, we obtain

$$\phi_h(b,t) - \phi_h(a,t) = \int_\Omega u_h(x,t)\,\mathrm{d}x.$$

Setting $c(t) = \int_\Omega u_h(x,t)\,\mathrm{d}x$, it follows from the above equality that

$$\begin{aligned}
\frac{\mathrm{d}}{\mathrm{d}t}c(t) = \int_\Omega (u_h)_t\,\mathrm{d}x &= -\int_\Omega (\varepsilon^2 u_h(u_h)_x + \eta(u_h)_{xxx})\,\mathrm{d}x\\
&= -\int_\Omega \left(\frac{\varepsilon^2}{2}u_h^2 + \eta(u_h)_{xx}\right)_x \mathrm{d}x = 0.
\end{aligned}$$

The last equality holds due to the periodic boundary condition imposed on u_h. Hence, $c(t)$ is a constant which shows that $(\phi_h(b,t))_t = (\phi_h(a,t))_t$. The discrete energy conservation law (37) for the LDG scheme applied to the KdV equation can be derived in the similar way to ones for the NLS equation. ■

Proposition 2.4: *With the periodic boundary condition, the solution of the LDG scheme* (36) *for the KdV equation satisfies the semi-discrete linear conservation law*

$$\frac{\mathrm{d}}{\mathrm{d}t}\int_\Omega u_h\,\mathrm{d}x = 0, \tag{41}$$

which is independent of the choice of numerical fluxes.

Proof: Setting the test function $\mu = 1$ in the first equation of (36) and summing up the result over j with the periodic boundary condition will lead to the conservation law (41). ■

3. Multisymplecticity of the fully discretized LDG schemes

In this section, we will investigate the multisymplecticity of the LDG discretizations (13) for the NLS equation and (36) for the KdV equation when the symplectic algorithm is applied as a time discretization. To make the statement more clear, we adopt the following matrix and vector forms.

3.1. Matrix–vector notations for the LDG method

We denote

$$U = (u_1^0, \ldots, u_1^k, \ldots, u_j^0, \ldots, u_j^k, \ldots, u_N^0, \ldots, u_N^k)^{\mathrm{T}},$$

where k represents the degree of the interpolation polynomial and N denotes the spatial grids. If we set the $k+1$ nodes in each element as a unit, we can reform U as

$$U = (\boldsymbol{u}_1^{\mathrm{T}}, \boldsymbol{u}_2^{\mathrm{T}}, \ldots, \boldsymbol{u}_N^{\mathrm{T}})^{\mathrm{T}},$$

and denote $U_j := \boldsymbol{u}_j = (u_j^0, \ldots, u_j^k)^{\mathrm{T}}$.

The corresponding mass matrix denoted by $\boldsymbol{A}$ is an N-block diagonal matrix which sub-matrix has the form

$$(\boldsymbol{A}^s)_{ij} = \frac{h}{2}\langle l_i, l_j\rangle = \frac{h}{2}\int_{-1}^{1} l_i(\tilde{x}) l_j(\tilde{x})\,\mathrm{d}\tilde{x}, \quad i,j = 0,1,\ldots,k$$

with $l_i(\tilde{x})$ being the shape function and $\tilde{x} \in [-1,1]$. It is obvious that $\boldsymbol{A}^s$ and $\boldsymbol{A}$ are symmetric. The corresponding stiffness matrix denoted by $\boldsymbol{B}$ is an N-block diagonal matrix which sub-matrix is given by

$$(\boldsymbol{B}^s)_{ij} = \langle l_i', l_j\rangle = \int_{-1}^{1} l_i'(\tilde{x}) l_j(\tilde{x})\,\mathrm{d}\tilde{x}, \quad i,j = 0,1,\ldots,k$$

with $l_i'(\tilde{x})$ being the first-order derivative with respect to $\tilde{x}$.

Next, we define the associated matrices for the flux term. It is known that the value of $(\hat{u}_h v^-)_{j+1/2} - (\hat{u}_h v^+)_{j-1/2}$ is not zero only when the test function v is taken as $l_0(\tilde{x})$ or $l_p(\tilde{x})$. For these two cases, the values are $-\widehat{(u_h)}_{j-1/2}$ or $\widehat{(u_h)}_{j+1/2}$. Imposing the periodic boundary condition, the corresponding matrices to the left, right and central fluxes have the following form:

$$U^- = \boldsymbol{C}^- U, \quad U^+ = \boldsymbol{C}^+ U, \quad U^c = \boldsymbol{C}^c U,$$

where

$$(\boldsymbol{C}^-)_{ij} = \begin{cases} 1, & i = j = \sigma(k+1), \quad \sigma = 1,2,\ldots,N, \\ -1, & i-1 = j = \sigma(k+1), \quad \sigma = 1,2,\ldots,N-1, \\ -1, & i = 1,\ j = N(k+1), \\ 0 & \text{otherwise}, \end{cases}$$

$$(\boldsymbol{C}^+)_{ij} = \begin{cases} -1, & i = j = \sigma(k+1)+1, \quad \sigma = 0,1,\ldots,N-1, \\ 1, & i = j-1 = \sigma(k+1), \quad \sigma = 1,2,\ldots,N-1, \\ 1, & i = N(k+1),\ j = 1, \\ 0 & \text{otherwise} \end{cases}$$

and $\boldsymbol{C}^c = (\boldsymbol{C}^- + \boldsymbol{C}^+)/2$. Denote $\boldsymbol{B}^+ = \boldsymbol{B} - \boldsymbol{C}^+$, $\boldsymbol{B}^- = \boldsymbol{B} - \boldsymbol{C}^-$ and $\boldsymbol{B}^c = \boldsymbol{B} - \boldsymbol{C}^c$, we have the following proposition.

Proposition 3.1: *The matrix $\boldsymbol{B}^c$ is skew-symmetric and $\boldsymbol{B}^+ = -(\boldsymbol{B}^-)^{\mathrm{T}}$ under the periodic boundary condition.*

Proof: Denote b_{ij} the element of the matrix $\boldsymbol{B}$. It is easy to check that b_{ij} has the following properties:

$$b_{ij} = \begin{cases} -b_{ji}, & i \neq j, \\ \dfrac{1}{2}, & i = j = \sigma(k+1), \qquad \sigma = 1, 2, \ldots, N, \\ -\dfrac{1}{2}, & i = j = \sigma(k+1)+1, \qquad \sigma = 0, 1, \ldots, N-1. \end{cases}$$

Thus, the expressions for $\boldsymbol{B}^+$ and $\boldsymbol{B}^-$ are

$$(\boldsymbol{B}^-)_{ij} = \begin{cases} -\dfrac{1}{2}, & i = j = \sigma(k+1), \qquad \sigma = 1, 2, \ldots, N, \\ -\dfrac{1}{2}, & i = j = \sigma(k+1)+1, \qquad \sigma = 0, 1, \ldots, N-1, \\ 1, & i - 1 = j = \sigma(k+1), \qquad \sigma = 1, 2, \ldots, N-1, \\ 1, & i = 1,\ j = N(k+1), \\ b_{ij} & \text{otherwise}, \end{cases}$$

$$(\boldsymbol{B}^+)_{ij} = \begin{cases} \dfrac{1}{2}, & i = j = \sigma(k+1), \qquad \sigma = 1, 2, \ldots, N, \\ \dfrac{1}{2}, & i = j = \sigma(k+1)+1, \qquad \sigma = 0, 1, \ldots, N-1, \\ -1, & i = j - 1 = \sigma(k+1), \qquad \sigma = 1, 2, \ldots, N-1, \\ -1, & i = N(k+1),\ j = 1, \\ b_{ij} & \text{otherwise}. \end{cases}$$

It is easy to check that $\boldsymbol{B}^+ = -(\boldsymbol{B}^-)^{\mathrm{T}}$ and $\boldsymbol{B}^c$ is skew-symmetric as $\boldsymbol{B}^c = (\boldsymbol{B}^- + \boldsymbol{B}^+)/2$. ■

In addition, we use $\mathcal{F}(U) = (\mathcal{F}_1^{\mathrm{T}}(U), \mathcal{F}_2^{\mathrm{T}}(U), \ldots, \mathcal{F}_N^{\mathrm{T}}(U))^{\mathrm{T}}$ to denote the vector form of the nonlinear term $F(u_h)$ which element $\mathcal{F}_j(U)$ has the form

$$\mathcal{F}_j(U) = \left(\frac{h}{2}\langle F(u_j^i l_i), l_0 \rangle, \frac{h}{2}\langle F(u_j^i l_i), l_1 \rangle, \ldots, \frac{h}{2}\langle F(u_j^i l_i), l_p \rangle \right)^{\mathrm{T}}.$$

Here, $u_j^i l_i$ denotes the Einstein summation $u_j^i l_i = \sum_{i=0}^{p} u_j^i l_i(\tilde{x})$.

3.2. Multisymplecticity of the fully discretized LDG scheme for the NLS equation

Using the matrix–vector representation introduced in the above subsection, we can rewrite the LDG discretization (13) for the NLS equation as

$$\begin{aligned} \frac{\mathrm{d}}{\mathrm{d}t}(\boldsymbol{A}^s Q_j) + \boldsymbol{B}^s V_j - (\boldsymbol{C}^v V)_j &= \mathcal{F}^1(P_j, Q_j), \\ -\frac{\mathrm{d}}{\mathrm{d}t}(\boldsymbol{A}^s P_j) + \boldsymbol{B}^s W_j - (\boldsymbol{C}^w W)_j &= \mathcal{F}^2(P_j, Q_j), \\ -\boldsymbol{B}^s P_j + (\boldsymbol{C}^p P)_j &= \boldsymbol{A}^s V_j, \\ -\boldsymbol{B}^s Q_j + (\boldsymbol{C}^q Q)_j &= \boldsymbol{A}^s W_j, \end{aligned} \tag{42}$$

where $\boldsymbol{C}^p, \boldsymbol{C}^q, \boldsymbol{C}^v$ and$\boldsymbol{C}^w$ are the undetermined flux matrices, $\mathcal{F}^1$ and $\mathcal{F}^2$ correspond to the nonlinear terms $\alpha \int_{I_j}(p_h^2+q_h^2)p_h\mu \,\mathrm{d}x$ and $\alpha \int_{I_j}(p_h^2+q_h^2)q_h\lambda \,\mathrm{d}x$, respectively,

For the purpose of discussing the multisymplecticity of the LDG scheme (42), we use the tool of exterior differential for a function. Assume if $f(u)$ is a smooth function, then $\mathrm{d}f(u)$ is defined by

$$\mathrm{d}f(u)=\sum_i \frac{\partial f}{\partial u_i}\mathrm{d}u_i.$$

Denote $\boldsymbol{B}^v=\boldsymbol{B}-\boldsymbol{C}^v, \boldsymbol{B}^w=\boldsymbol{B}-\boldsymbol{C}^w, \boldsymbol{B}^p=\boldsymbol{B}-\boldsymbol{C}^p$ and $\boldsymbol{B}^q=\boldsymbol{B}-\boldsymbol{C}^q$. Taking the exterior derivative on both sides of Equation (42) gives

$$\begin{aligned}
\frac{\mathrm{d}}{\mathrm{d}t}(\boldsymbol{A}^s\,\mathrm{d}Q_j)+(\boldsymbol{B}^v\,\mathrm{d}V)_j&=\mathrm{d}\mathcal{F}^1(P_j,Q_j),\\
-\frac{\mathrm{d}}{\mathrm{d}t}(\boldsymbol{A}^s\,\mathrm{d}P_j)+(\boldsymbol{B}^w\,\mathrm{d}W)_j&=\mathrm{d}\mathcal{F}^2(P_j,Q_j),\\
-(\boldsymbol{B}^p\,\mathrm{d}P)_j&=\boldsymbol{A}^s\,\mathrm{d}V_j,\\
-(\boldsymbol{B}^q\,\mathrm{d}Q)_j&=\boldsymbol{A}^s\,\mathrm{d}W_j,
\end{aligned}\tag{43}$$

The exterior differentials of the nonlinear terms $\mathcal{F}_1$ and $\mathcal{F}_1$ are computed by

$$\begin{aligned}
\mathrm{d}\mathcal{F}^1(P_j,Q_j)&=L^s_{p+q}\,\mathrm{d}P_j+L^s_{pq}\,\mathrm{d}Q_j+L^s_p\,\mathrm{d}P_j,\\
\mathrm{d}\mathcal{F}^2(P_j,Q_j)&=L^s_{p+q}\,\mathrm{d}Q_j+L^s_{pq}\,\mathrm{d}P_j+L^s_q\,\mathrm{d}Q_j,
\end{aligned}\tag{44}$$

where, L^s_{p+q}, L^s_{pq}, L^s_p, and L^s_q are all symmetric matrices and defined as follows:

$$\begin{aligned}
(L^s_{p+q})_{m,n}&=\frac{h\alpha}{2}\int_{-1}^{1} l_m l_n[(p_j^i l_i)^2+(q_j^i l_i)^2]\,\mathrm{d}\tilde{x},\\
(L^s_{pq})_{m,n}&=h\alpha\int_{-1}^{1} l_m l_n(p_j^i l_i)(q_j^i l_i)\,\mathrm{d}\tilde{x},\quad m,n=0,1,\ldots,k,\\
(L^s_p)_{m,n}&=h\alpha\int_{-1}^{1} l_m l_n(p_j^i l_i)^2\,\mathrm{d}\tilde{x},\quad (L^s_q)_{m,n}=h\alpha\int_{-1}^{1} l_m l_n(q_j^i l_i)^2\,\mathrm{d}\tilde{x}.
\end{aligned}$$

Taking the wedge product of the variational equations (43) on both sides with dP_j, $\mathrm{d}Q_j$, $\mathrm{d}V_j$, $\mathrm{d}W_j$, respectively, we derive

$$\begin{aligned}
\mathrm{d}P_j\wedge\frac{\mathrm{d}}{\mathrm{d}t}(\boldsymbol{A}^s\,\mathrm{d}Q_j)+\mathrm{d}P_j\wedge(\boldsymbol{B}^v\,\mathrm{d}V)_j&=\mathrm{d}P_j\wedge L^s_{pq}\,\mathrm{d}Q_j,\\
-\mathrm{d}Q_j\wedge\frac{\mathrm{d}}{\mathrm{d}t}(\boldsymbol{A}^s\,\mathrm{d}P_j)+\mathrm{d}Q_j\wedge(\boldsymbol{B}^w\,\mathrm{d}W)_j&=\mathrm{d}Q_j\wedge L^s_{pq}\,\mathrm{d}P_j,\\
-\mathrm{d}V_j\wedge(\boldsymbol{B}^p\,\mathrm{d}P)_j&=0,\\
-\mathrm{d}W_j\wedge(\boldsymbol{B}^q\,\mathrm{d}Q)_j&=0.
\end{aligned}\tag{45}$$

Summing up the four equations in (45) and using the symmetry of L^s_{pq}, we obtain N semi-discrete multisymplectic conservation laws

$$\frac{\mathrm{d}}{\mathrm{d}t}(\mathrm{d}P_j\wedge\boldsymbol{A}^s\,\mathrm{d}Q_j)+[\mathrm{d}P_j\wedge(\boldsymbol{B}^v\,\mathrm{d}V)_j+(\boldsymbol{B}^p\,\mathrm{d}P)_j\wedge\,\mathrm{d}V_j+dQ_j\wedge(\boldsymbol{B}^w\,\mathrm{d}W)_j+(\boldsymbol{B}^q\,\mathrm{d}Q)_j\wedge\,\mathrm{d}W_j]=0,\tag{46}$$

for $j=1,2,\ldots,N$.

Remark 3.1: Notice that for the conventional multisymplectic schemes generated from the finite difference or pseudo-spectral method, the corresponding multisymplectic conservation laws hold at each node. However, for the LDG method, this conservation law (46) is valid at the element j instead of at the node P_j^i, $i = 0, 1, \ldots, k$ for example, which has significant difference with those of all known methods.

If we choose the numerical flux as that in (23), we can further get the conservation of the total symplecticity over time by summing up the above equation for j from 1 to N and using the results of Proposition 3.1, that is

$$\frac{\mathrm{d}}{\mathrm{d}t}(\mathrm{d}P \wedge \boldsymbol{A}\,\mathrm{d}Q) = 0.$$

Due to the symplectic property inherited by the above semi-discretized system, it is naturally to apply a symplectic integration to discretize the system (42) in time. We adopt the mid-point rule and obtain

$$\begin{aligned}
\boldsymbol{A}^s\frac{Q_j^{n+1}-Q_j^n}{\tau} + (\boldsymbol{B}^- V^{n+1/2})_j &= \mathcal{F}^1(P_j^{n+1/2}, Q_j^{n+1/2}),\\
-\boldsymbol{A}^s\frac{P_j^{n+1}-P_j^n}{\tau} + (\boldsymbol{B}^- W^{n+1/2})_j &= \mathcal{F}^2(P_j^{n+1/2}, Q_j^{n+1/2}),\\
-(\boldsymbol{B}^+ P^{n+1/2})_j &= \boldsymbol{A}^s V_j^{n+1/2},\\
-(\boldsymbol{B}^+ Q^{n+1/2})_j &= \boldsymbol{A}^s W_j^{n+1/2},
\end{aligned} \tag{47}$$

where $P^{n+1/2} = (P^{n+1} + P^n)/2$, etc. Analogously, we can derive the fully discrete version of the multisymplectic conservation law for the numerical discretization (47)

$$\begin{aligned}
&\frac{1}{\tau}(\mathrm{d}P_j^{n+1} \wedge \boldsymbol{A}^s\,\mathrm{d}Q_j^{n+1} - \mathrm{d}P_j^n \wedge \boldsymbol{A}^s\,\mathrm{d}Q_j^n) + [\mathrm{d}P_j^{n+1/2} \wedge (\boldsymbol{B}^-\mathrm{d}V)_j^{n+1/2} + (\boldsymbol{B}^+\mathrm{d}P)_j^{n+1/2} \wedge \mathrm{d}V_j^{n+1/2},\\
&\quad + \mathrm{d}Q_j^{n+1/2} \wedge (\boldsymbol{B}^-\mathrm{d}W)_j^{n+1/2} + (\boldsymbol{B}^+\mathrm{d}Q)_j^{n+1/2} \wedge \mathrm{d}W_j^{n+1/2}] = 0.
\end{aligned} \tag{48}$$

Summing up the index j, we have the global symplectic conservation law

$$\mathrm{d}P^{n+1} \wedge \boldsymbol{A}\,\mathrm{d}Q^{n+1} = \mathrm{d}P^n \wedge \boldsymbol{A}\,\mathrm{d}Q^n. \tag{49}$$

From the above analysis, it is known that the LDG scheme (47) is multisymplectic. Further eliminating the auxiliary variables V and W in Equation (47), we can obtain the final numerical scheme in a general form

$$\begin{aligned}
\boldsymbol{A}\frac{Q^{n+1}-Q^n}{\tau} - \boldsymbol{B}^v\boldsymbol{A}\boldsymbol{B}^p P^{n+1/2} &= \mathcal{F}^1(P^{n+1/2}, Q^{n+1/2}),\\
-\boldsymbol{A}\frac{P^{n+1}-P^n}{\tau} - \boldsymbol{B}^w\boldsymbol{A}\boldsymbol{B}^q Q^{n+1/2} &= \mathcal{F}^2(P^{n+1/2}, Q^{n+1/2}).
\end{aligned} \tag{50}$$

where $\boldsymbol{B}^p$, $\boldsymbol{B}^v$, $\boldsymbol{B}^q$, and $\boldsymbol{B}^w$ are determined by the concrete choice of numerical flux. For the numerical flux (23), we have

$$\boldsymbol{B}^p = \boldsymbol{B}^+, \quad \boldsymbol{B}^v = \boldsymbol{B}^-, \quad \boldsymbol{B}^q = \boldsymbol{B}^+, \quad \boldsymbol{B}^w = \boldsymbol{B}^-$$

Table 1. Spatial accuracy of real part of solution by the scheme MS-NLS-LDGI.

	N	L^2 error	Order	L^∞ error	Order
p^1	80	4.11E−02	–	2.80E−01	–
	160	1.16E−02	1.83	7.63E−02	1.88
	320	2.98E−03	1.95	1.97E−02	1.95
	640	7.45E−04	2.00	4.90-03	2.01
p^2	40	4.25E−02	–	2.09E−01	–
	80	6.03E−03	2.82	4.57E−02	2.20
	160	7.93E−04	2.92	6.29E−03	2.86
	320	1.02E−04	2.95	7.88E−04	3.00
p^3	40	1.00E−02	–	6.90E−02	–
	80	7.22E−04	3.79	6.98E−03	3.31
	160	4.09E−05	4.14	3.82E−04	4.19
	320	2.46E−06	4.05	2.55E−05	3.91

Table 2. Spatial accuracy of imaginary part of solution by the scheme MS-NLS-LDGI.

	N	L^2 error	Order	L^∞ error	Order
p^1	80	3.76E−02	–	1.98E−01	–
	160	1.09E−02	1.78	6.96E−02	1.51
	320	2.80E−03	1.96	1.87E−02	1.89
	640	6.99E−04	2.00	4.72E−03	1.99
p^2	40	2.78E−02	–	1.65E−01	
	80	6.04E−03	2.20	4.30E−02	1.94
	160	7.93E−04	2.93	6.11E−03	2.82
	320	1.02E−04	2.96	8.35E−04	2.87
p^3	40	1.10E−03	–	8.04E−02	–
	80	6.65E−04	4.05	5.39E−03	3.90
	160	4.07E−05	4.03	4.77E−04	3.50
	320	2.45E−06	4.06	3.00E−05	3.99

Table 3. Spatial accuracy of real part of solution by the scheme MS-NLS-LDGIII.

	N	L^2 error	Order	L^∞ error	Order
p^1	80	6.65E−02	–	5.30E−01	–
	160	2.42E−02	1.46	1.96E−01	1.43
	320	9.45E−03	1.35	6.97E−02	1.49
	640	4.27E−03	1.15	2.68E−02	1.38
p^2	80	2.15E−02	–	9.81E−02	–
	160	6.92E−04	4.96	3.95E−03	4.64
	320	7.93E−05	3.12	4.77E−04	3.05
	640	1.01E−05	2.98	6.77E−05	2.81
p^3	40	1.89E−02	–	5.82E−02	–
	80	6.04E−04	4.96	4.07E−03	3.84
	160	5.77E−05	3.38	4.65E−04	3.13
	320	7.67E−06	2.91	5.65E−05	3.04

and the corresponding scheme is denoted as MS-NLS-LDGI. For numerical flux (24), we have

$$\boldsymbol{B}^p = \boldsymbol{B}^-, \quad \boldsymbol{B}^v = \boldsymbol{B}^+, \quad \boldsymbol{B}^q = \boldsymbol{B}^-, \quad \boldsymbol{B}^w = \boldsymbol{B}^+$$

and the corresponding scheme is denoted as MS-NLS-LDGII. For numerical flux (25), we have

$$\boldsymbol{B}^p = \boldsymbol{B}^c, \quad \boldsymbol{B}^v = \boldsymbol{B}^c, \quad \boldsymbol{B}^q = \boldsymbol{B}^c, \quad \boldsymbol{B}^w = \boldsymbol{B}^c$$

and the corresponding scheme is denoted as MS-NLS-LDGIII. Notice that the three schemes can all admit the corresponding fully discrete charge conservation.

Table 4. Spatial accuracy of imaginary part of solution by the scheme MS-NLS-LDGIII.

	N	L^2 error	Order	L^∞ error	Order
p^1	80	6.41E−02	–	5.15E−01	–
	160	2.33E−02	1.46	1.84E−01	1.48
	320	9.27E−03	1.33	7.14E−02	1.37
	640	4.24E−03	1.13	2.80E−02	1.35
p^2	80	2.13E−02	–	8.09E−02	–
	160	6.92E−04	4.94	4.14E−03	4.29
	320	7.93E−05	3.13	4.88E−04	3.08
	640	1.01E−05	2.98	7.23E−05	2.75
p^3	40	1.86E−02	–	8.57E−02	–
	80	5.58E−04	5.06	3.13E−03	4.78
	160	5.80E−05	3.27	4.15E−04	2.91
	320	7.70E−06	2.91	5.85E−05	2.83

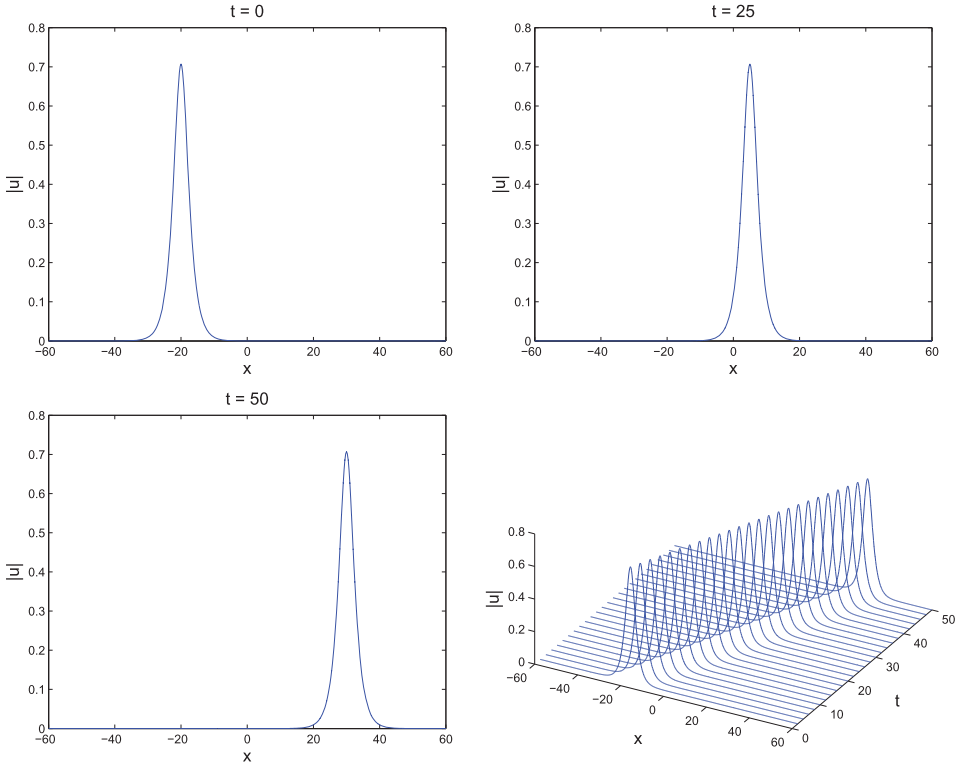

Figure 1. Single soliton propagation with the initial condition (76).

Proposition 3.2: *The schemes MS-NLS-LDGI, MS-NLS-LDGII, and MS-NLS-LDGIII for the NLS equation exactly preserve the charge conservation law, i.e.*

$$\frac{1}{2}\int_\Omega [(p_h^{n+1})^2 + (q_h^{n+1})^2]\,\mathrm{d}x = \frac{1}{2}\int_\Omega [(p_h^{n})^2 + (q_h^{n})^2]\,\mathrm{d}x. \tag{51}$$

Proof: Applying the mid-point rule to (13) in time direction and taking the test functions as $\mu = (q_h)^{n+1/2}$, $\lambda = -(p_h)^{n+1/2}$, $\xi = (w_h)^{n+1/2}$, $\nu = -(v_h)^{n+1/2}$, and combining the resulting

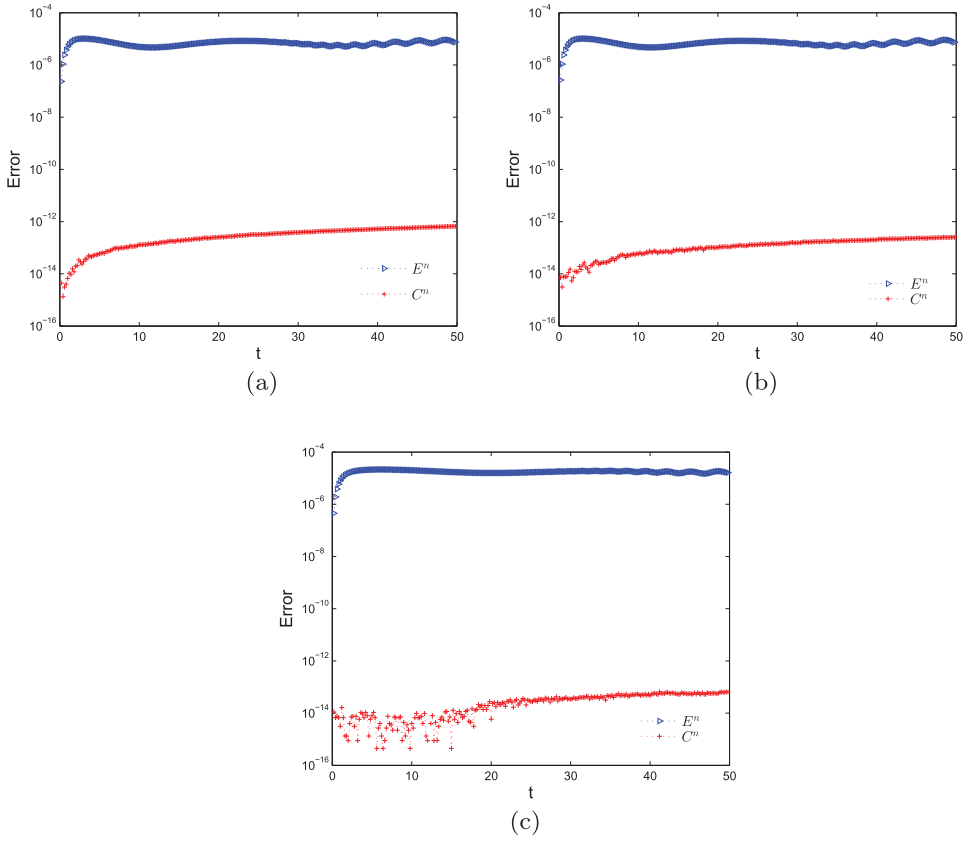

Figure 2. Errors in the discrete energy and charge. (a) By scheme MS-NLS-LDGI; (b) By scheme MS-NLS-LDGII; and (c) By scheme MS-NLS-LDGIII.

equations lead to

$$\begin{aligned}
&\frac{1}{2\tau}\left(\int_{I_j}[(p_h^{n+1})^2+(q_h^{n+1})^2]\,\mathrm{d}x-\int_{I_j}[(p_h^{n})^2+(q_h^{n})^2]\,\mathrm{d}x\right)\\
&\quad=-(v_h^- q_h^-)_{j+1/2}^{n+1/2}+(v_h^+ q_h^+)_{j-1/2}^{n+1/2}+(w_h^- p_h^-)_{j+1/2}^{n+1/2}-(w_h^+ p_h^+)_{j-1/2}^{n+1/2}\\
&\qquad+(\hat{v}_h q_h^-)_{j+1/2}^{n+1/2}-(\hat{v}_h q_h^+)_{j-1/2}^{n+1/2}+(\hat{q}_h v_h^-)_{j+1/2}^{n+1/2}-(\hat{q}_h v_h^+)_{j-1/2}^{n+1/2}\\
&\qquad-(\hat{w}_h p_h^-)_{j+1/2}^{n+1/2}+(\hat{w}_h p_h^+)_{j-1/2}^{n+1/2}-(\hat{p}_h w_h^-)_{j+1/2}^{n+1/2}+(\hat{p}_h w_h^+)_{j-1/2}^{n+1/2},
\end{aligned}$$

here, the discrete integration by part has been used. Summing up the above equation over j and using one of Equations (23)–(25) as the numerical flux provides that the right-hand side terms vanish. This completes the proof of this theorem. ■

Corollary 3.1: *The schemes MS-NLS-LDGI, MS-NLS-LDGII and MS-NLS-LDGIII for the NLS equation are unconditionally stable in the L^2-norm.*

3.3. Multisymplecticity of the full-discrete LDG scheme for the KdV equation

Similar to the above discussion for the NLS equation, in this section we study the LDG discretization for the KdV equation by combining the corresponding time integrator. The semi-discretized LDG

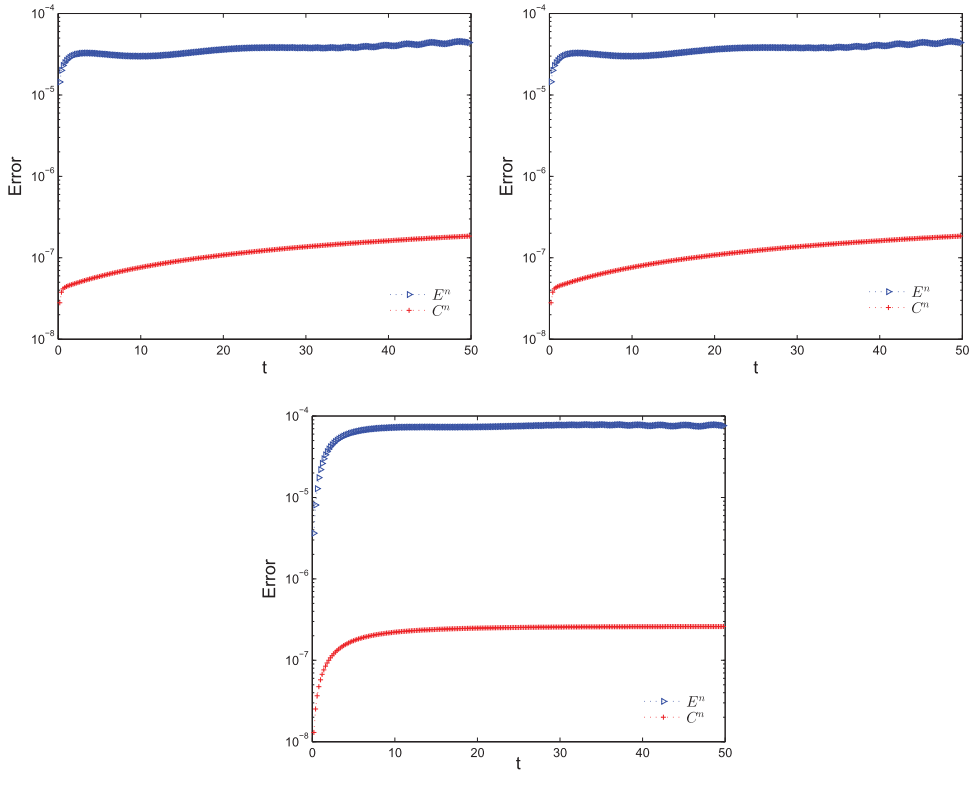

Figure 3. Errors in the discrete energy and charge by the TVD Runge–Kutta method.

scheme (36) for the KdV equation can be reformed by using the matrix–vector expression

$$\begin{aligned} \frac{1}{2}\frac{\mathrm{d}}{\mathrm{d}t}\boldsymbol{A}^s U_j - (\boldsymbol{B}^w W)_j &= 0, \\ -\frac{1}{2}\frac{\mathrm{d}}{\mathrm{d}t}\boldsymbol{A}^s \Phi_j + \varepsilon(\boldsymbol{B}^v V)_j &= -\boldsymbol{A}^s W_j + \mathcal{F}(U_j), \\ -\varepsilon(\boldsymbol{B}^u U)_j &= \boldsymbol{A}^s V_j, \\ (\boldsymbol{B}^\phi \Phi)_j &= -\boldsymbol{A}^s U_j, \end{aligned} \tag{52}$$

where $\mathcal{F}(U_j)$ corresponds to the nonlinear term $\eta/2\int_{I_j}(u_h)^2\,\mathrm{d}x$.

Next, we discuss the multisymplecticity of the LDG scheme (52) for the KdV equation. The exterior derivative of $\mathcal{F}(U)$ is calculated by

$$\mathrm{d}\mathcal{F}(U_j) = L_u^s\,\mathrm{d}U_j, \tag{53}$$

where L_u^s is symmetric and defined as

$$(L_u^s)_{m,n} = \frac{h\eta}{2}\int_{-1}^{1} l_m l_n (u_j^i l_i)\,\mathrm{d}\tilde{x}, \quad m,n = 0,1,\ldots,k.$$

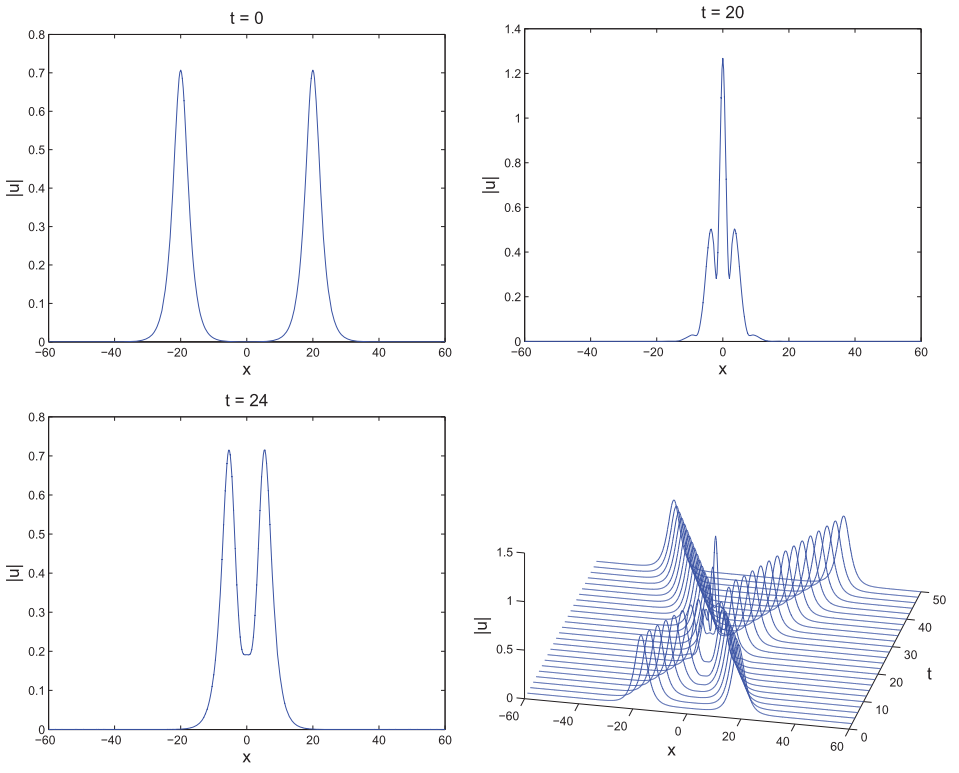

Figure 4. Double-soliton collision with the initial condition (76).

Taking the wedge product on the variational equations of (52) with $\mathrm{d}\Phi_j$, $\mathrm{d}U_j$, $\mathrm{d}V_j$, $\mathrm{d}W_j$, respectively, we obtain

$$\begin{aligned}
\frac{1}{2}\mathrm{d}\Phi_j \wedge \frac{\mathrm{d}}{\mathrm{d}t}\boldsymbol{A}^s\,\mathrm{d}U_j - \mathrm{d}\Phi_j \wedge (\boldsymbol{B}^w\,\mathrm{d}W)_j &= 0,\\
-\frac{1}{2}\mathrm{d}U_j \wedge \frac{\mathrm{d}}{\mathrm{d}t}\boldsymbol{A}^s\,\mathrm{d}\Phi_j + \varepsilon\,\mathrm{d}U_j \wedge (\boldsymbol{B}^v\,\mathrm{d}V)_j &= -\mathrm{d}U_j \wedge \boldsymbol{A}^s\,\mathrm{d}W_j,\\
-\varepsilon\,\mathrm{d}V_j \wedge (\boldsymbol{B}^u\,\mathrm{d}U)_j &= 0,\\
\mathrm{d}W_j \wedge (\boldsymbol{B}^\phi\,\mathrm{d}\Phi)_j &= -\mathrm{d}W_j \wedge \boldsymbol{A}^s\,\mathrm{d}U_j,
\end{aligned} \tag{54}$$

where we have used the symmetricity of $\boldsymbol{A}^s$ and L_u^s. Summing up the above four equations gives N semi-discrete multisymplectic conservation law

$$\begin{aligned}
&\frac{1}{2}\frac{\mathrm{d}}{\mathrm{d}t}(\mathrm{d}\Phi_j \wedge \boldsymbol{A}^s\,\mathrm{d}U_j) + [\mathrm{d}W_j \wedge (\boldsymbol{B}^\phi\,\mathrm{d}\Phi)_j + (\boldsymbol{B}^w\,\mathrm{d}W)_j \wedge\,\mathrm{d}\Phi_j\\
&\quad + \varepsilon\,\mathrm{d}U_j \wedge (\boldsymbol{B}^v\,\mathrm{d}V)_j + \varepsilon(\boldsymbol{B}^u\,\mathrm{d}U)_j \wedge\,\mathrm{d}V_j] = 0,
\end{aligned} \tag{55}$$

for $j = 1, 2, \ldots, N$.

If we take the numerical flux as that in Proposition 2.3 and consider the matrix properties in Proposition 3.1 we can obtain the conservation of the global symplecticity by summing up Equation (55) over j, which yields

$$\frac{\mathrm{d}}{\mathrm{d}t}(\mathrm{d}\Phi \wedge \boldsymbol{A}\,\mathrm{d}U) = 0.$$

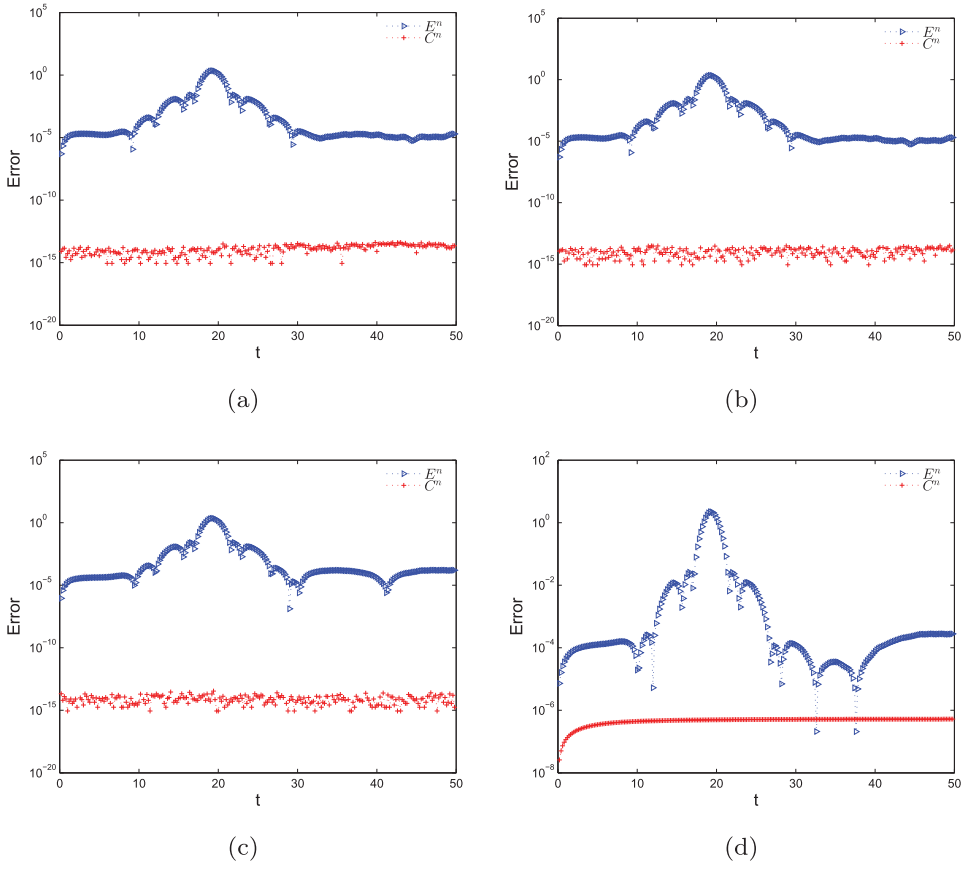

Figure 5. Errors in the discrete energy and charge. (a) By MS-NLS-LDGI; (b) By MS-NLS-LDGII; (c) By MS-NLS-LDGIII; and (d) By TVD Runge–Kutta method.

Also applying the mid-point rule to discretize (52), we get the following scheme:

$$\frac{1}{2}\boldsymbol{A}^s\frac{U_j^{n+1}-U_j^n}{\tau}-(\boldsymbol{B}^w W^{n+1/2})_j=0, \tag{56}$$

$$-\frac{1}{2}\boldsymbol{A}^s\frac{\Phi_j^{n+1}-\Phi_j^n}{\tau}+\varepsilon(\boldsymbol{B}^v V^{n+1/2})_j=-\boldsymbol{A}^s W_j^{n+1/2}+\mathcal{F}(U_j^{n+1/2}), \tag{57}$$

$$-\varepsilon(\boldsymbol{B}^u U^{n+1/2})_j=\boldsymbol{A}^s V^{n+1/2}, \tag{58}$$

$$(\boldsymbol{B}^\phi \Phi^{n+1/2})_j=-\boldsymbol{A}^s U^{n+1/2}, \tag{59}$$

which can be proved to admit the following multisymplectic conservation law

$$\begin{aligned}&\frac{1}{2\tau}(\mathrm{d}\Phi_j^{n+1}\wedge\boldsymbol{A}^s\,\mathrm{d}U_j^{n+1}-\mathrm{d}\Phi_j^n\wedge\boldsymbol{A}^s\,\mathrm{d}U_j^n)+[\mathrm{d}W_j^{n+1/2}\wedge(\boldsymbol{B}^\phi\,\mathrm{d}\Phi)_j^{n+1/2}\\&\quad+(\boldsymbol{B}^w\,\mathrm{d}W)_j^{n+1/2}\wedge\mathrm{d}\Phi_j^{n+1/2}+\varepsilon\,\mathrm{d}U_j^{n+1/2}\wedge(\boldsymbol{B}^v\,\mathrm{d}V)_j^{n+1/2}+\varepsilon(\boldsymbol{B}^u\,\mathrm{d}U)_j^{n+1/2}\wedge\mathrm{d}V_j^{n+1/2}]=0.\end{aligned} \tag{60}$$

Table 5. Spatial accuracy for the scheme MS-KdV-LDGI.

	N	L^2 error	Order	L^∞ error	Order
p^1	50	1.37E−01	–	4.94E−01	–
	100	1.49E−02	3.20	8.93E−02	2.47
	200	3.30E−03	2.18	2.14E−02	2.06
	400	7.12E−04	2.21	5.38E−03	1.99
p^2	50	1.26E−02	–	7.83E−02	–
	100	1.06E−03	3.56	7.66E−03	3.35
	200	1.17E−04	3.18	1.12E−03	2.78
	400	1.30E−05	3.17	1.36E−04	3.03
p^3	25	2.28E−02	–	7.23E−02	–
	50	1.30E−03	4.13	1.25E−02	2.53
	100	6.56E−05	4.31	6.46E−04	4.27
	200	4.21E−06	3.96	5.71E−05	3.51

Table 6. Space accuracy test for the scheme MS-KdV-LDGIII.

	N	L^2 error	Order	L^∞ error	Order
p^1	50	5.78E−02	–	3.17E−01	–
	100	2.42E−02	1.26	1.17E−01	1.44
	200	1.24E−03	0.96	6.18E−02	0.92
	400	6.33E−03	0.97	2.70E−02	1.19
p^2	50	3.05E−02	–	1.10E−01	–
	100	1.38E−03	4.46	7.33E−03	3.91
	200	7.83E−05	4.14	6.10E−04	3.59
	400	9.03E−06	3.12	7.03E−05	3.12
p^3	25	3.48E−02	–	1.25E−01	–
	50	1.36E−03	4.68	7.70E−03	4.02
	100	9.42E−05	3.85	7.33E−04	3.39
	200	1.11E−05	3.09	8.38E−05	3.13

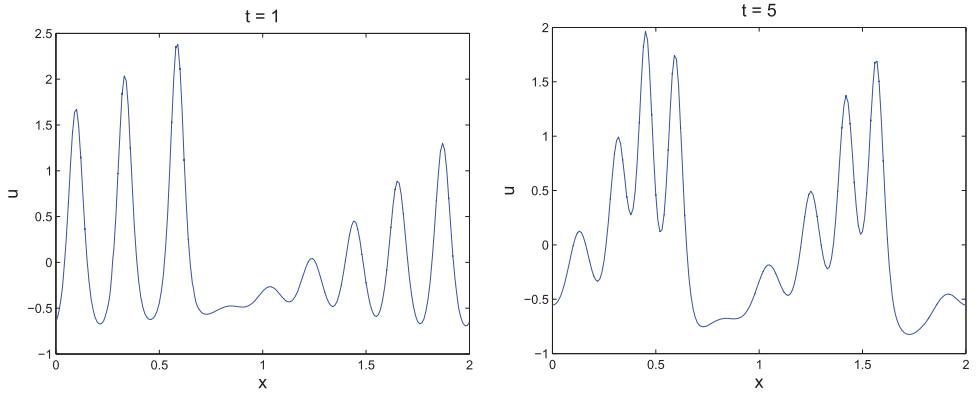

Figure 6. Snapshots of wave profiles at $t = 1$ and $t = 5$ by schemes MS-KdV-LDGI or MS-KdV-LDGII.

Summing up for j, the global symplectic conservation is obtained

$$\mathrm{d}\Phi^{n+1} \wedge \boldsymbol{A}\,\mathrm{d}U^{n+1} = \mathrm{d}\Phi^{n} \wedge \boldsymbol{A}\,\mathrm{d}U^{n}. \tag{61}$$

Hence, we derive a multisymplectic LDG scheme for the KdV equation. Notice that in the above derivation, we have not specifically chosen the numerical flux yet because we need to further consider the solvability of the resulting algebraic system (56)–(59), not just the request of energy conservation

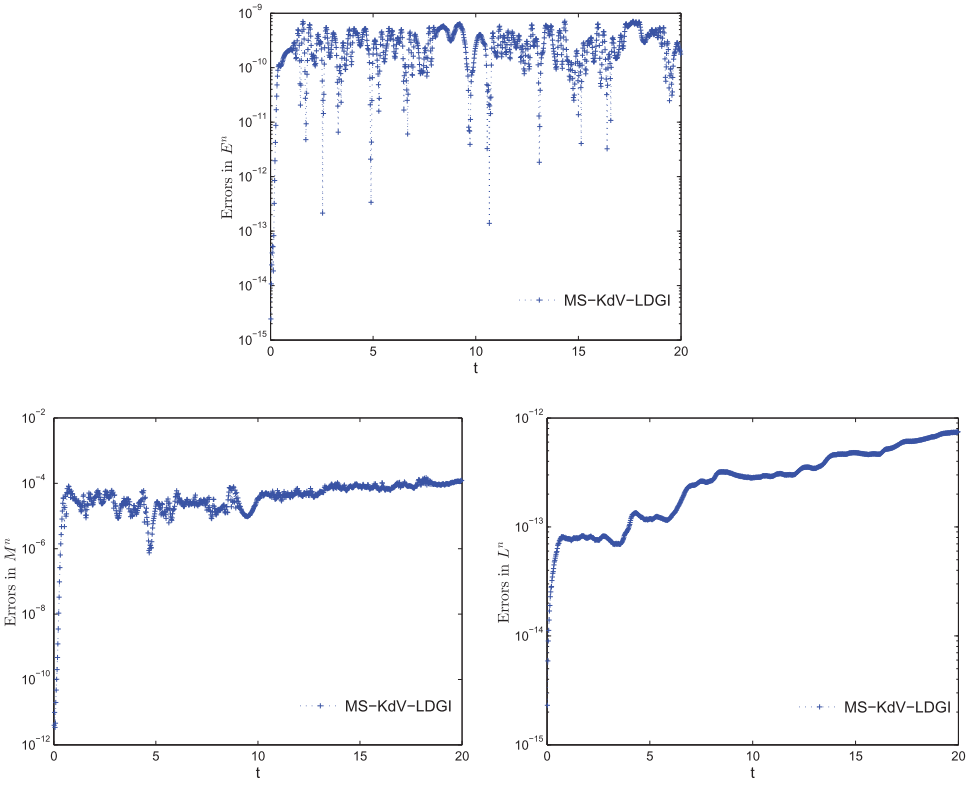

Figure 7. Errors in the discrete invariants E^n, M^n, and L^n by the scheme MS-KdV-LDGI.

in Proposition 2.3. In the following, we will present another restriction on the choice of numerical fluxes.

Unlike the LDG scheme (47) applied to the NLS equation, constructing the LDG schemes for the KdV equation needs to consider an extra equation of the potential ϕ introduced for reformulating the multisymplectic formulation of the KdV equation. Notice that the matrices $\boldsymbol{B}^-$, $\boldsymbol{B}^+$ and $\boldsymbol{B}^c$ are all degenerated, thus no matter which kind of matrices $\boldsymbol{B}^\phi$ are taken, Equation (59) defines an underdetermined system. At the very beginning about the solvability of the multisymplectic Preissmann scheme for the KdV equation [31], authors also encountered this problem and proved that the value of Φ can vary with a constant which does not affect the desired solution of U. More precisely, if we fix one component of Φ to a constant, the system (56)–(59) can be resolved.

In contrast to the technique in [31], we provide another simple approach to solve the system (56)–(59) due to the multiple choice of numerical fluxes. Denote the difference operators as

$$\delta_t^+ U^n = \frac{U^{n+1} - U^n}{\tau}, \quad \delta_t U^n = U^{n+1/2} = \frac{U^{n+1} + U^n}{2}.$$

We then assemble the sub-system (56)–(59) into the entire system about Φ, U, V, W in the operator form

$$\begin{aligned} \tfrac{1}{2}\boldsymbol{A}\delta_t^+ U^n - \boldsymbol{B}^w \delta_t W^n &= 0, \\ -\tfrac{1}{2}\boldsymbol{A}\delta_t^+ \Phi^n + \varepsilon \boldsymbol{B}^v \delta_t V^n &= -\boldsymbol{A}\delta_t W^n + \mathcal{F}(\delta_t U^n), \\ -\varepsilon \boldsymbol{B}^u \delta_t U^n &= \boldsymbol{A}\delta_t V^n, \\ \boldsymbol{B}^\phi \delta_t \Phi^n &= -\boldsymbol{A}\delta_t U^n, \end{aligned} \tag{62}$$

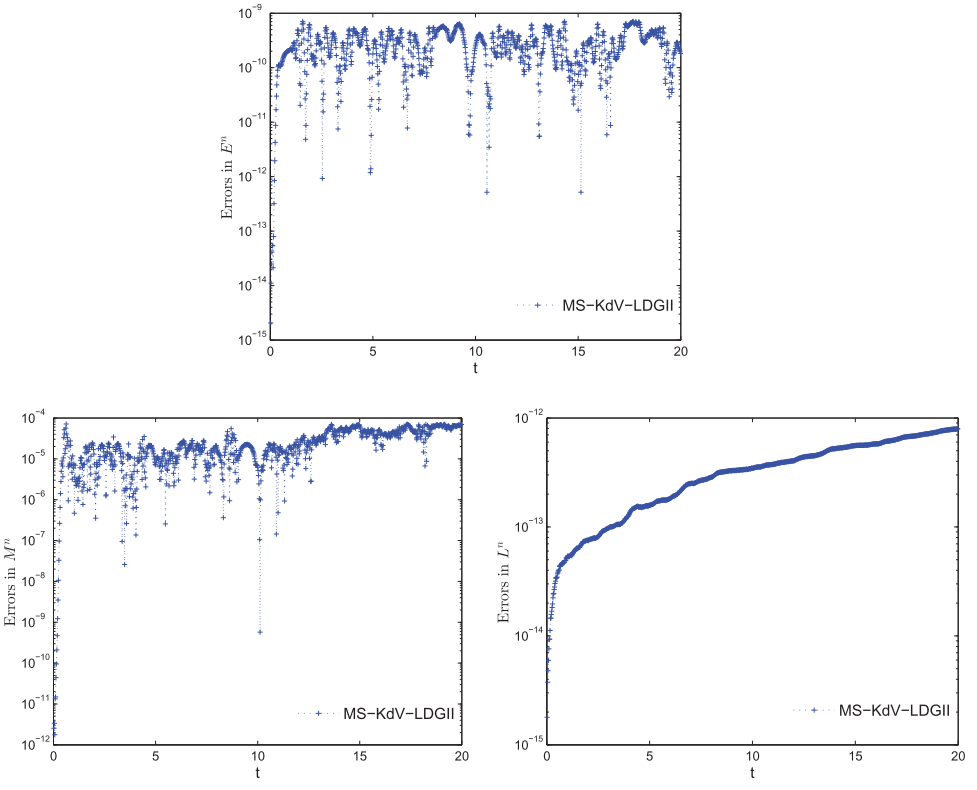

Figure 8. Errors in the discrete invariants E^n, M^n, and L^n by the scheme MS-KdV-LDGII.

which is equivalent to the following reduced system:

$$\tfrac{1}{2}\boldsymbol{A}\delta_t^+ U^n - \boldsymbol{B}^w \delta_t W^n = 0, \tag{63}$$

$$-\tfrac{1}{2}\boldsymbol{A}\delta_t^+ \Phi^n + \varepsilon \boldsymbol{B}^v \delta_t V^n = -\boldsymbol{A}\delta_t W^n + \mathcal{F}(\delta_t U^n), \tag{64}$$

$$-\varepsilon \boldsymbol{B}^u U^n = \boldsymbol{A} V^n, \tag{65}$$

$$\boldsymbol{B}^\phi \Phi^n = -\boldsymbol{A} U^n, \tag{66}$$

according to the result in [1]. Multiplying $\boldsymbol{B}^\phi \boldsymbol{A}^{-1}$ on Equation (64) and substituting the relation of Equations (65) and (66), we obtain

$$\tfrac{1}{2}\boldsymbol{A}\delta_t^+ U^n - \varepsilon^2 \boldsymbol{B}^\phi \boldsymbol{A}^{-1}\boldsymbol{B}^v \boldsymbol{A}^{-1}\boldsymbol{B}^u \delta_t U^n = -\boldsymbol{B}^\phi \delta_t W^n + \boldsymbol{B}^\phi \boldsymbol{A}^{-1}\mathcal{F}(\delta_t U^n). \tag{67}$$

However, we cannot further eliminate the intermediate variable W^n since $\boldsymbol{B}^w$ is not invertible and incommutable with $\boldsymbol{B}^\phi$. The key of our method is to choose the same flux for the variables ϕ_h and w_h which yields the following proposition.

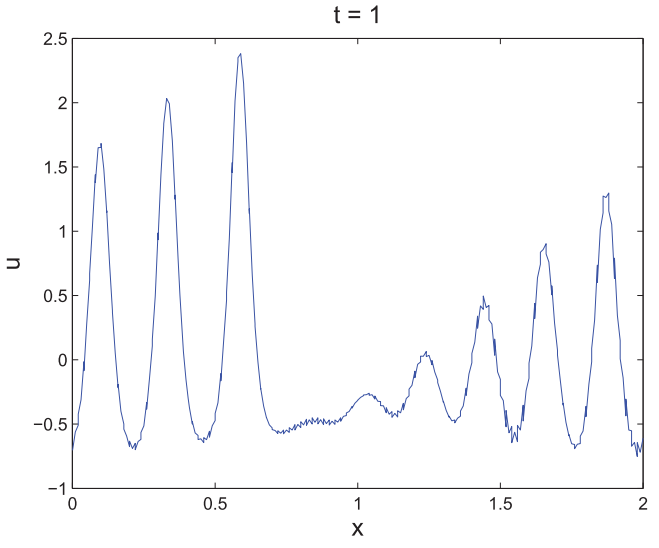

Figure 9. Snapshot of the wave profile at $t = 1$ by the scheme MS-KdV-LDGIII.

Proposition 3.3: *To fulfil the semi-discrete energy conservation law* (37) *and eliminate all the intermediate variables, we can only choose three sets of the numerical flux for the multisymplectic LDG scheme* (63)–(66), *namely*

$$\hat{u}_h = u_h^+, \quad \hat{v}_h = v_h^-, \quad \hat{\phi}_h = \phi_h^c, \quad \hat{w}_h = w_h^c, \tag{68}$$

$$\hat{u}_h = u_h^-, \quad \hat{v}_h = v_h^+, \quad \hat{\phi}_h = \phi_h^c, \quad \hat{w}_h = w_h^c, \tag{69}$$

or

$$\hat{u}_h = u_h^c, \quad \hat{v}_h = v_h^c, \quad \hat{\phi}_h = \phi_h^c, \quad \hat{w}_h = w_h^c. \tag{70}$$

Proof: Consider Equations (63) and (67), the remaining intermediate variable W can be eliminated if and only if $\boldsymbol{B}^w = \boldsymbol{B}^\phi$, i.e. the same choice of fluxes for w_h and ϕ_h. Moreover, based on the request of the semi-discrete energy conservation law, one can only take the central flux for both w_h and ϕ_h, which results the above three kinds of numerical fluxes. ■

For example, if we take the fluxes as Equation (68), the corresponding multisymplectic scheme is

$$\boldsymbol{A}\delta_t^+ U^n - \varepsilon^2 \boldsymbol{B}^c \boldsymbol{A}^{-1} \boldsymbol{B}^- \boldsymbol{A}^{-1} \boldsymbol{B}^+ \delta_t U^n = \boldsymbol{B}^c \boldsymbol{A}^{-1} \mathcal{F}(\delta_t U^n). \tag{71}$$

Similarly, with the other two choices of numerical fluxes (69) and (70) the LDG discetizations also lead to multisymplectic schemes

$$\boldsymbol{A}\delta_t^+ U^n - \varepsilon^2 \boldsymbol{B}^c \boldsymbol{A}^{-1} \boldsymbol{B}^+ \boldsymbol{A}^{-1} \boldsymbol{B}^- \delta_t U^n = \boldsymbol{B}^c \boldsymbol{A}^{-1} \mathcal{F}(\delta_t U^n), \tag{72}$$

and

$$\boldsymbol{A}\delta_t^+ U^n - \varepsilon^2 \boldsymbol{B}^c \boldsymbol{A}^{-1} \boldsymbol{B}^c \boldsymbol{A}^{-1} \boldsymbol{B}^c \delta_t U^n = \boldsymbol{B}^c \boldsymbol{A}^{-1} \mathcal{F}(\delta_t U^n). \tag{73}$$

We denote the above three LDG schemes by MS-KdV-LDGI, MS-KdV-LDGII, and MS-KdV-LDGIII, respectively.

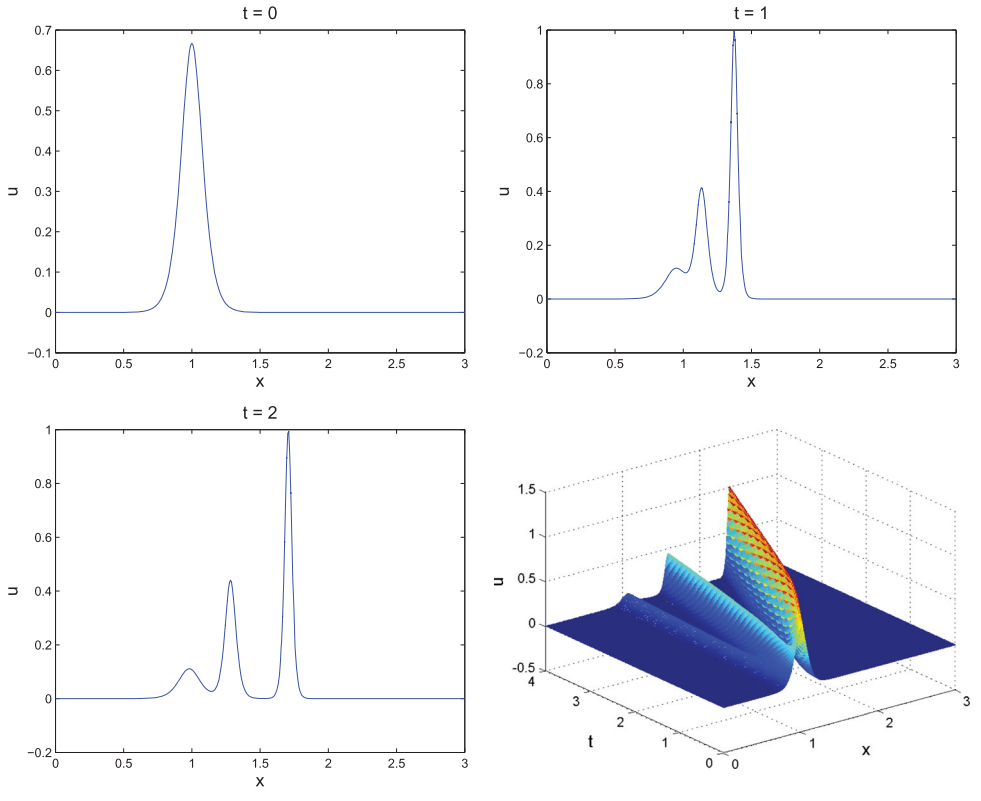

Figure 10. Triple soliton profiles with initial condition (80).

Proposition 3.4: *The schemes MS-KdV-LDGI, MS-KdV-LDGII, and MS-KdV-LDGIII for the KdV equation exactly preserve the linear conservation law, i.e.*

$$\int_\Omega u_h^{n+1}\,\mathrm{d}x = \int_\Omega u_h^n\,\mathrm{d}x. \tag{74}$$

Proof: Applying the mid-point rule on the first equation of (36), setting the test function $\mu = 1$ and summing up the resulting equality over j with the periodic boundary condition will lead to the conservation law (74). ■

We cannot strictly prove the fully discrete energy and momentum conservation laws, but the numerical results on the errors of conservative quantities are demonstrated in the numerical experiments.

4. Numerical experiments

In this section, we present the numerical tests computed by the multisymplectic LDG schemes developed as above to illustrate the accuracy of numerical solutions and error of numerical invariants. We start this section by defining the discrete energies E^n for the NLS and the KdV equations as

$$E^n = \frac{1}{2}\int_\Omega \left(\frac{\alpha}{2}((p_h^n)^2 + (q_h^n)^2) - (v_h^n)^2 - (w_h^n)^2\right)\mathrm{d}x,$$

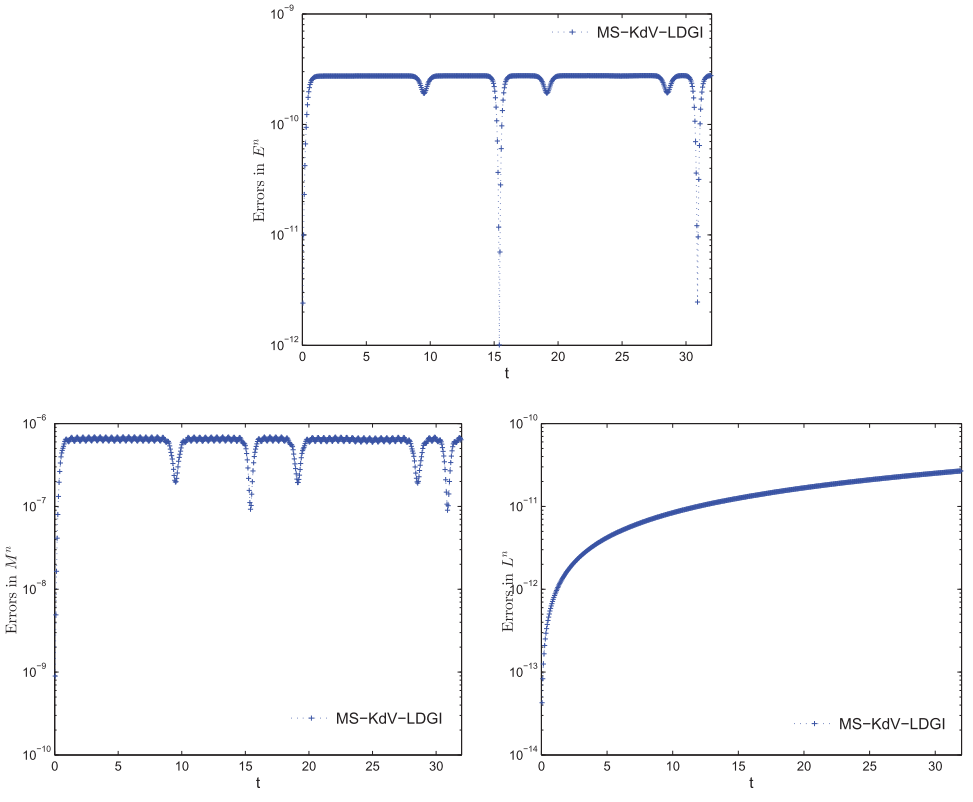

Figure 11. Errors in the discrete invariants E^n, M^n and L^n by the scheme MS-KdV-LDGI.

and

$$E^n = \int_\Omega \left(\frac{\eta}{6}(u_h^n)^3 - \frac{1}{2}(v_h^n)^2 \right) \mathrm{d}x.$$

The discrete charge C^n for the NLS equation, the discrete momentum M^n and linear invariant L^n for the KdV equation are defined as

$$C^n = \frac{1}{2}\int_\Omega ((p_h^n)^2 + (q_h^n)^2)\,\mathrm{d}x,$$
$$M^n = \frac{1}{2}\int_\Omega (u_h^n)^2\,\mathrm{d}x, \quad L^n = \int_\Omega u_h\,\mathrm{d}x,$$

respectively.

4.1. Numerical examples for the NLS equation

Example 4.1: Consider the NLS equation defined on $[-25, 25]$. When $\alpha = 2$, the equation has a soliton solution which is expressed as

$$u(x,t) = \mathrm{sech}(x - 4t)\exp\left(2\mathrm{i}\left(x - \frac{3}{2}t\right)\right). \tag{75}$$

With the exact solution (75), we present an accuracy test for the schemes MS-NLS-LDGI, MS-NLS-LDGII, and MS-NLS-LDGIII. In Tables 1 and 2, we give the errors of numerical solutions in L^2

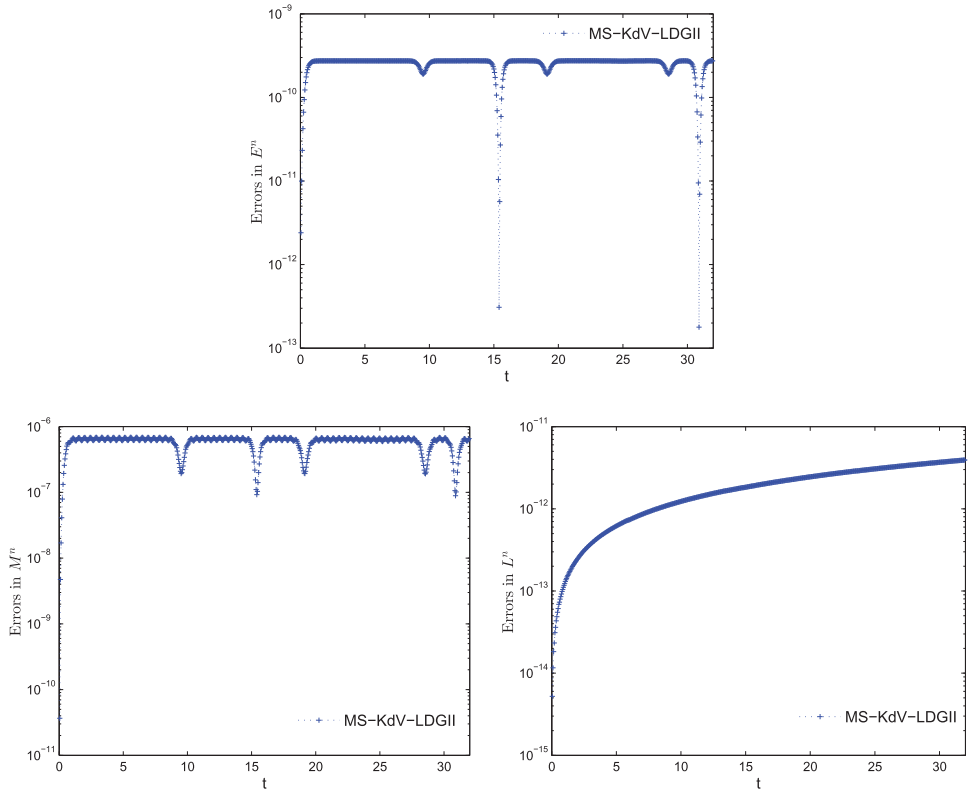

Figure 12. Errors in the discrete invariants E^n, M^n and L^n by the scheme MS-KdV-LDGII.

and L^∞ norms and the numerical order of accuracy for the scheme MS-NLS-LDGI. The $(k+1)$th order of accuracy in both norms can be investigated for the numerical discretizations with P^k $(k \leq 3)$ elements. Here, we omit the similar results given by the scheme MS-NLS-LDGII.

The scheme MS-NLS-LDGIII is constructed with the central fluxes. The numerical discretization as pointed in [12] usually provides a numerical solution with only a suboptimal order k rather than the expected order $k+1$ for odd k. The numerical results exhibited in Tables 3 and 4 coincide with the theoretical results.

Example 4.2: In this example, we consider the soliton propagation with the initial condition

$$u(x,0) = \frac{\sqrt{2}}{2}\operatorname{sech}\left(\frac{x+p}{2}\right)\exp\left(\mathrm{i}\frac{x+p}{2}\right), \tag{76}$$

where p is the initial phase. The problem is solved over $[-60, 60]$ with $\alpha = 1$ and $p = 20$. The P^2 element with 240 uniform meshes and $\tau = 0.001$ are taken hereafter for solving the NLS equation. In Figure 1, we show the soliton propagation with the envelope or the modulus of $|u(x,t)|$ which can be simulated well by all three schemes even after a very long time. The corresponding errors of the discrete energy and charge are presented in Figure 2. We can see that all the methods can preserve the charge invariant up to the machine precision because the fluxes used for constructing these numerical methods satisfy the condition presented in Corollary 2.1. It is also shown that they can preserve the energy very well.

We compare the above multisymplectic LDG methods with a total variation diminishing (TVD) RK-DG method which is presented in [35] by using the TVD Runge–Kutta methods in time. In

Figure 3, we illustrate the errors of discrete energy and charge produced by the LDG scheme equipped with the TVD Runge–Kutta method and one of the numerical fluxes (23)–(25). Although the resulting schemes have excellent behaviours in stability and computational efficiency, the errors in the discrete charge show a linear growth and the magnitudes of the errors are much larger than that of the corresponding multisymplectic LDG schemes in Figure 2.

Example 4.3: We consider the interaction of two solitons with the initial value

$$u(x,0) = \frac{\sqrt{2}}{2}\left[\operatorname{sech}\left(\frac{x+p}{2}\right)\exp\left(\mathrm{i}\frac{x+p}{2}\right) + \operatorname{sech}\left(\frac{x-p}{2}\right)\exp\left(-\mathrm{i}\frac{x-p}{2}\right)\right]. \tag{77}$$

In such case, the initial phases of two solitary waves are symmetric about origin with equal amplitudes and opposite velocities. The solution is computed over $[-60, 60]$ till $t = 50$ with $p = 20$. Figure 4 presents the snapshots as well as the wave propagation of the two solitons which can be well resolved by all three multisymplectic schemes. Errors in the energy and charge by these schemes and the TVD Runge–Kutta time discretization with fluxes (23) are shown in Figure 5. From Figure 5 (a)–(c), it can be seen that all the methods can preserve the charge up to the round-off errors and also can bound the energy besides the collision moment. In comparison, with the TVD Runge–Kutta method in time the numerical method performs a larger errors in energy.

4.2. Numerical examples for the KdV equation

It is discussed as above, the implementation of the LDG method for the KdV equation is different from ones for the NLS equation. In this section, we present the numerical experiments for the KdV equation.

Example 4.4: In order to see the accuracy of the multisymplectic LDG methods MS-KdV-LDGI, MS-KdV-LDGII, and MS-KdV-LDGIII, we apply these numerical methods to the KdV equation with $\eta = 6, \varepsilon = 1$ defined on $[-20, 20]$. The exact solution of this KdV equation is

$$u(x,t) = 2\operatorname{sech}^2(x - 4t). \tag{78}$$

The problem is solved till $t = 0.5$. Tables 5 and 6 show the numerical errors and order of accuracy for the schemes MS-KdV-LDGI and MS-KdV-LDGIII. We omit the result of the scheme MS-KdV-LDGII which is close to that of scheme MS-KdV-LDGI. It is observed that schemes MS-KdV-LDGI and MS-KdV-LDGII can illustrate the numerical solutions with an optimal order $k+1$ as we take the central flux for variables ϕ_h, w_h, and choose the alternative flux for variables u_h and v_h. For the scheme MS-KdV-LDGIII which uses the central fluxes for all variables, the numerical solution can only reach a suboptimal order which is k in this test.

Example 4.5: In this example, we test the three conservative schemes for the KdV equation with a classic initial value introduced by Zabusky and Kruskal [37]

$$u(x,0) = \cos(\pi x), \tag{79}$$

where $\eta = 1$, $\varepsilon = 0.022$ and the computation domain is $[0, 2]$. The P^2 element with 100 uniform meshes and $\tau = 2E - 5$ are taken in this example. The wave profiles at $t = 1$ and $t = 5$ are presented in Figure 6 which are simulated by the multisymplectic schemes MS-KdV-LDGI or MS-KdV-LDGII. The errors of discrete conservation laws of these schemes are plotted in Figures 7 and 8, respectively, which demonstrates that both schemes can preserve the energy E^n and momentum M^n very well. Since the momentum here is a positive quantity, the long-term stability of numerical schemes can be guaranteed from the preservation of this invariant. For the linear conservation law L^n, both schemes

exhibit a round-off error that coincides with our theoretical result. However, the scheme MS-KdV-LDGIII with the same element and mesh grid fails to simulate the wave propagation which can be seen from Figure 9. To improve the numerical result produced by scheme MS-KdV-LDGIII, we need use a fine mesh. This concludes that for this case the schemes MS-KdV-LDGI and MS-KdV-LDGII are more efficient than the scheme MS-KdV-LDGIII as the former two schemes are more accurate. Therefore in our next example, we omit the test for the scheme MS-KdV-LDGIII.

Example 4.6: Consider the triple soliton case with the initial condition

$$u(x,0) = \frac{2}{3}\mathrm{sech}^2\left(\frac{x-1}{\sqrt{108\epsilon}}\right), \tag{80}$$

where $\eta = 1, \epsilon = 10^{-4}$. The computation domain is taken as $[0, 3]$. The P^2 element with 200 uniform meshes and $\tau = 5\mathrm{E}-5$ are taken in this example. Figure 10 plots the wave profiles produced by the scheme MS-KdV-LDGI or MS-KdV-LDGII. It is clear that the splitting process is well resolved and the three new appeared solitons can be observed clearly. Errors in the discrete conservation laws are illustrated in Figures 11 and 12 for the two schemes over a long-time interval. It illustrates a slight difference from each other.

5. Concluding remarks

This paper proposes a new framework to construct the LDG scheme for PDEs which can be written in multisymplectic formulation. Taking the NLS and the KdV equations as examples, we present the corresponding LDG spatial discretizations based on their multisymplectic formulations. By choosing specially the numerical fluxes, we have proved that the resulting LDG discretizations for both equations naturally admit a corresponding semi-discretized energy conservation law. In addition, the LDG scheme for the NLS equation preserves not only a semi-discretized charge conservation law, but also a full-discrete version when the symplectic mid-point rule is used in time and the periodic boundary condition is applied. For KdV equation, we also prove that the linear conservation law can be precisely preserved with all choices of numerical flux mentioned in this paper. Furthermore, we study the multisymplecticity of the obtained schemes which usually help to ensure the stability and long-time simulations of the given numerical methods. In numerical experiments, the comparison of the conservative multisymplectic LDG schemes in terms of order of accuracy, soliton propagation and invariant preservation is given.

Note

1. Let $\mathcal{N}$ be an operator on the Banach space. The symmetry condition means $\mathcal{N}'_u = \tilde{\mathcal{N}}'_u$, where

$$\mathcal{N}'_u\psi = \lim_{\epsilon\to 0}\frac{\mathcal{N}(u+\epsilon\psi)-\mathcal{N}(u)}{\epsilon} = \frac{\mathrm{d}}{\mathrm{d}\epsilon}\mathcal{N}(u+\epsilon\psi)\Big|_{\epsilon=0},$$

and $\tilde{\mathcal{N}}'_u$ is the adjoint of $\mathcal{N}'_u$. For the KdV equation, $\mathcal{N}(u) = u_t + \eta u u_x + \varepsilon^2 u_{xxx}$ which does not satisfy the symmetry condition.

Disclosure statement

No potential conflict of interest was reported by the authors.

Funding

This research work was currently supported by National Basic Research Program of China (2014 CB845906), the ITER-China Program (2014GB124005), National Natural Science Foundation of China under (grant nos. 41274103, 11271195, 11321061, 11271357, 41504078).

ORCID

W. Cai http://orcid.org/0000-0002-6149-3780

References

[1] U.M. Ascher and R.I. McLachlan, *On symplectic and multisymplectic schemes for the KdV equation*, J. Sci. Comput. 25 (2005), pp. 83–104.

[2] J.L. Bona, H. Chen, O. Karakashian, and Y. Xing, *Conservative, discontinuous-Galerkin methods for the generalized Korteweg–de Vries equation*, Math. Comput. 82 (2013), pp. 1401–1432.

[3] T.J. Bridges and S. Reich, *Multi-symplectic integrators: Numerical schemes for Hamiltonian PDEs that conserve symplecticity*, Phys. Lett. A 284 (2001), pp. 184–193.

[4] T.J. Bridges and S. Reich, *Multi-symplectic spectral discretizations for the Zakharov–Kuznetsov and shallow water equations*, Phys. D 152–153 (2001), pp. 491–504.

[5] T.J. Bridges and S. Reich, *Numerical methods for Hamiltonian PDEs*, J. Phys. A: Math. Gen. 39 (2006), pp. 5287–5320.

[6] J. Cai, Y. Wang, and Z. Qiao, *Multisymplectic Preissman scheme for the time-domain Maxwell's equations*, J. Math. Phys. 50 (2009). doi:10.1063/1.3087421

[7] W. Cai, Y. Sun, and Y. Wang, *Variational discretizations for the generalized Rosenau-type*, Appl. Math. Comput. 271 (2015), pp. 860–873.

[8] J. Chen and M. Qin, *Multi-symplectic Fourier pseudospectral method for the nonlinear Schrödinger equation*, Electon. Trans. Numer. Anal. 12 (2001), pp. 193–204.

[9] P. Ciarlet, *The Finite Element Method for Elliptic Problems*, SIAM, Philadelphia, 2002.

[10] B. Cockburn and C.-W. Shu, *TVB Runge–Kutta local projection discontinuous Galerkin finite element method for conservation laws II: General framework*, Math. Comput. 52 (1989), pp. 411–435.

[11] B. Cockburn and C.-W. Shu, *The Runge–Kutta discontinuous Galerkin method for conservation laws V: Multidimensional systems*, J. Comput. Phys. 141 (1998), pp. 199–224.

[12] B. Cockburn and C.-W. Shu, *The local discontinuous Galerkin method for time-dependent convection–diffusion systems*, SIAM J. Numer. Anal. 35 (1998), pp. 2440–2463.

[13] B. Cockburn, S.-Y. Lin, and C.-W. Shu, *TVB Runge–Kutta local projection discontinuous Galerkin finite element method for conservation laws III: One dimensional systems*, J. Comput. Phys 84 (1989), pp. 90–113.

[14] B. Cockburn, S. Hou, and C.-W. Shu, *The Runge–Kutta local projection discontinuous Galerkin finite element method for conservation laws IV: The multidimensional case*, Math. Comput. 54 (1990), pp. 548–581.

[15] D. Cohen, B. Owren, and X. Raynaud, *Multi-symplectic integration of the Camassa–Holm equation*, J. Comput. Phys. 227 (2008), pp. 5492–5512.

[16] J. Frank, B.E. Moore, and S. Reich, *Linear PDEs and numerical methods that preserve a multisymplectic conservation law*, SIAM J. Sci. Comput. 28 (2006), pp. 260–277.

[17] Y. Gong, J. Cai, and Y. Wang, *Some new structure-preserving algorithms for general multi-symplectic formulations of Hamiltonian PDEs*, J. Comput. Phys. 279 (2014), pp. 80–102.

[18] E. Hairer, C. Lubich, and G. Wanner, *Geometric Numerical Integration: Structure-Preserving Algorithms for Ordinary Differential Equations*, 2nd ed., Springer, Berlin, 2006.

[19] J. Hong, H. Liu, and G. Sun, *The multi-symplecticity of partitioned Runge–Kutta methods for Hamiltonian PDEs*, Math. Comput. 75 (2005), pp. 167–182.

[20] A.L. Islas, D.A. Karpeev, and C.M. Schober, *Geometric integrators for the nonlinear Schrödinger equation*, J. Comput. Phys. 173 (2001), pp. 116–148.

[21] L. Kong, J. Hong, and J. Zhang, *Splitting multisymplectic integrators for Maxwell's equations*, J. Comput. Phys. 229 (2010), pp. 4259–4278.

[22] H. Liu and Y. Xing, *An invariant preserving discontinuous Galerkin method for the Camassa–Holm equation*, SIAM J. Sci. Comput. 38 (2016), pp. A1919–A1934.

[23] H. Liu and N. Yi, *A Hamiltonian preserving discontinuous Galerkin method for the generalized Korteweg–de Vries equation*, J. Comput. Phys. 321 (2016), pp. 776–796.

[24] J.E. Marsden, G.P. Patrick, and S. Shkoller, *Multisymplectic geometry, variational integrators, and nonlinear PDEs*, Commun. Math. Phys. 199 (1998), pp. 351–395.

[25] W.H. Reed and T.R. Hill, *Triangular mesh methods for the neutron transport equation*, Technical Report Tech. report LA-UR-73-479, Los Alamos Scientic Laboratory, 1973.

[26] S. Reich, *Multi-symplectic Runge–Kutta collocation methods for Hamiltonian wave equations*, J. Comput. Phys 157 (1999), pp. 473–499.

[27] J.-Q. Sun and M.-Z. Qin, *Multi-symplectic methods for the coupled 1D nonlinear Schrödinger system*, Comput. Phys. Commun. 155 (2003), pp. 221–235.

[28] Y. Sun and P.S.P. Tse, *Symplectic and multisymplectic numerical methods for Maxwell's equations*, J. Comput. Phys. 230 (2011), pp. 2076–2094.

[29] W. Tang, Y. Sun, and W. Cai, *Discontinuous Galerkin methods for Hamiltonian ODEs and PDEs*, J. Comput. Phys. 330 (2017), pp. 340–364.
[30] M.M. Vainberg, *Variational Methods for the Study of Nonlinear Operators*, Holden-Day, San Francisco, CA, 1964. Translated by A. Feinstein.
[31] Y. Wang, B. Wang, and M. Qin, *Numerical implementation of the multisymplectic Preissman scheme and its equivalent schemes*, Appl. Math. Comput. 149 (2004), pp. 299–326.
[32] Y. Xia and Y. Xu, *A conservative local discontinuous Galerkin method for the Schrödinger–KdV system*, Commun. Comput. Phys. 15 (2014), pp. 1091–1107.
[33] Y. Xu and C.-W. Shu, *Local discontinuous Galerkin methods for nonlinear Schrödinger equations*, J. Comput. Phys. 205 (2005), pp. 72–97.
[34] Y. Xu and C.-W. Shu, *Local discontinuous Galerkin methods for high-order time dependent partial differential equations*, Commun. Comput. Phys. 7 (2010), pp. 1–46.
[35] J. Yan and C.-W. Shu, *A local discontinuous Galerkin method for KdV type equations*, SIAM J. Numer. Anal. 40 (2002), pp. 769–791.
[36] N. Yi, Y. Huang, and H. Liu, *A direct discontinuous Galerkin method for the generalized Korteweg'de Vries equation: Energy conservation and boundary effect*, Commun. Comput. Phys. 242 (2013), pp. 351–366.
[37] N.J. Zabusky and M.D. Kruskal, *Interaction of "solitons" in a collisionless plasma and the recurrence of initial states*, Phys. Rev. Lett. 15 (1965), pp. 240–243.
[38] P.F. Zhao and M.Z. Qin, *Multisymplectic geometry and multisymplectic Preissmann scheme for the KdV equation*, J. Phys. A – Math. Gen. 33 (2000), pp. 3613–3626.
[39] H. Zhu, L. Tang, S. Song, Y. Tang, and D. Wang, *Symplectic wavelet collocation method for Hamiltonian wave equations*, J. Comput. Phys. 229 (2010), pp. 2550–2572.
[40] H. Zhu, S. Song, and Y. Tang, *Multi-symplectic wavelet collocation method for the nonlinear Schrödinger equation and the Camassa–Holm equation*, Comput. Phys. Commun. 182 (2012), pp. 616–627.